

AD-A179 342

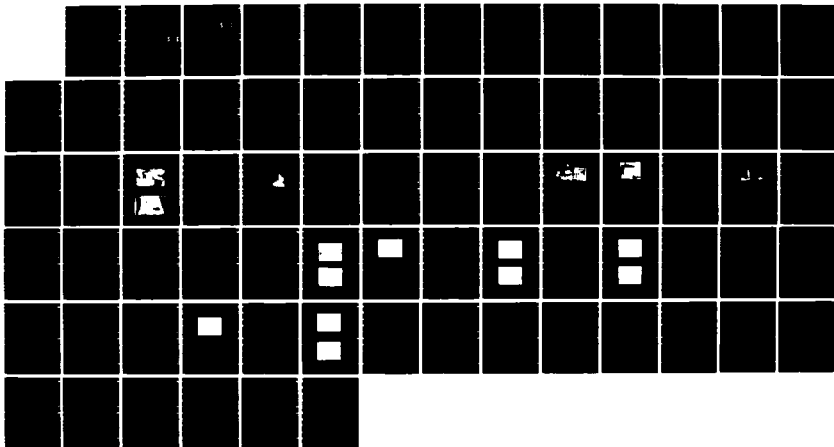
BOUNDARY LAYER DISTURBANCES CAUSED BY PERIODIC HEATING
OF A THIN RIBBON(U) AIR FORCE INST OF TECH
WRIGHT-PATTERSON AFB OH SCHOOL OF ENGINEERING
L KUDELKA DEC 86 AFIT/GAE/AA/86D-7

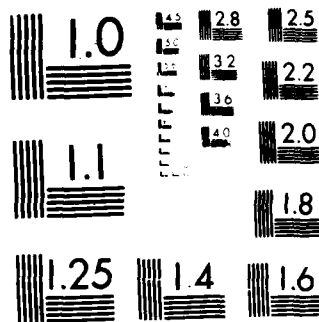
1/1

UNCLASSIFIED

F/G 28/4

NL





MICROCOPY RESOLUTION TEST CHART
NATIONAL BUREAU OF STANDARDS-1963-A

DTIC FILE COPY

1

AD-A179 342



DTIC
 ELECTE
 APR 17 1987
 S D

BOUNDARY LAYER DISTURBANCES
 CAUSED BY PERIODIC HEATING
 OF A THIN RIBBON

THESIS

Lawrence Kudelka
 Captain, USAF

AFIT/GAE/AA/86D-7

DISTRIBUTION STATEMENT A
 Approved for public release
 Distribution Unlimited

DEPARTMENT OF THE AIR FORCE
 AIR UNIVERSITY
AIR FORCE INSTITUTE OF TECHNOLOGY

Wright-Patterson Air Force Base, Ohio

87 4 16 023

AFIT/GAE/AA/86D-7

DTIC
EL
APR 17 1987
S D

BOUNDARY LAYER DISTURBANCES
CAUSED BY PERIODIC HEATING
OF A THIN RIBBON

THESIS

Lawrence Kudelka
Captain, USAF

AFIT/GAE/AA/86D-7

Approved for public release; distribution unlimited.

AFIT/GAE/AA/86D-7

BOUNDARY LAYER DISTURBANCES CAUSED BY
PERIODIC HEATING OF A THIN RIBBON

THESIS

Presented to the Faculty of the School of Engineering
of the Air Force Institute of Technology

Air University

In Partial Fulfillment of the
Requirements for the Degree of
Master of Science in Aeronautical Engineering



Lawrence Kudelka, B.S.
Captain, USAF

December 1986

Accession For		
NTIS	CRA&I	M
DTIC	TAB	U
Unannounced		U
Justification		
By		
Distribution/		
Availability Codes		
Dist	Availability or Special	
A-1		

Approved for public release; distribution unlimited.

Preface

Disturbances in a laminar boundary layer are subtle phenomena. Detecting and stimulating these waves was more challenging than I expected it would be when I started. I've gained an appreciation for the skill of the professional scientists whose works appear in my bibliography. They make it look easy, but at every turn, reality waits for the innocent experimenter.

Several people provided invaluable assistance to me. Mr. Joe Hofele, of the AFIT Model Shop, accurately converted the pictures in my mind into wind tunnel models. Mr. Nick Yardich, Lab Supervisor, obtained the equipment I needed and offered useful suggestions. Technician Jay Anderson performed magic with electronic components and enabled me to effectively take data. Also, I thank my advisor, Dr. Milton Franke, for his patience and his guidance throughout this project.

Finally, I thank my wife Diann and daughter Jacqui for their love, support, and encouragement during the long days and nights of study.

Lawrence Kudelka

This thesis was prepared on a Commodore 128 using "Word Writer 128" by Timeworks. The printer was a Panasonic KX-P1091.

Table of Contents

	Page
Preface	ii
List of Figures	iv
List of Symbols	vi
Abstract	vii
I. Introduction	1
Background	1
Objective and Scope	5
II. Theory	7
Disturbances in Laminar Flow	7
Temperature Response of Ribbon	10
III. Experimental Apparatus and Procedure	16
Apparatus for Preliminary Experiment	16
Apparatus and Procedure in 14-in Wind Tunnel	18
Apparatus and Procedure in 9-in Wind Tunnel	25
IV. Results and Discussion	33
Heating Element Characteristics	33
Vibration of Ribbon	34
14-in Wind Tunnel Results	36
9-in Wind Tunnel Results	38
Alternative Causes of Velocity Fluctuations	47
Heating Without Vibration	49
V. Conclusions and Recommendations	57
Conclusions	57
Recommendations	58
Bibliography	60
Vita	62

List of Figures

<u>Figure</u>		<u>Page</u>
1.	Estimated theoretical response of Nichrome ribbon to pulsed voltage	11
2.	Arrangement of equipment for test of heating element response to pulsed voltage	17
3.	Equipment arrangement at 14-in Wind Tunnel .	19
4.	Equipment at 14-in Wind Tunnel	20
5.	Flat plate in test section of 14-in tunnel .	20
6.	Boundary layer hot film probe, TSI Model 1218-20	22
7.	Calibration curve for anemometer output . .	24
8.	Equipment arrangement at 9-in Wind Tunnel. .	26
9.	Equipment at 9-in Wind Tunnel	27
10.	Flat plate in test section of 9-in tunnel, with boundary layer hot film probe and temperature sensor	28
11.	Section of flat plate A for use in 9-in tunnel	30
12.	Configurations of flat plates	31
13.	Free stream turbulence in 14-in tunnel . . .	37
14.	Boundary layer disturbances without heating.	37
15.	Periodic heating of ribbon in 14-in tunnel .	38
16.	Boundary layer in 9-in tunnel, no heat . . .	40
17.	Periodic heating of ribbon, $y=0.005$ in . . .	40
18.	Periodic heating of ribbon, $y=0.06$ in . . .	42
19.	Periodic heating of ribbon, $y=0.08$ in . . .	42
20.	Dimensionless velocity profile	43
21.	Turbulence profile, vibrating ribbon	45

<u>Figure</u>		<u>Page</u>
22.	Relative amplitude vs pulse frequency	46
23.	Anemometer response with no flow	49
24.	Boundary layer, no heat	51
25.	Periodic heating of non-vibrating ribbon	51
26.	Turbulence profile, no heat	52
27.	Turbulence profile, pulsed heat	53
28.	Dimensionless velocity profile, no heat	54
29.	Dimensionless velocity, pulsed heat	55

List of Symbols

<u>Symbol</u>		<u>Units</u>
C_E	Coefficient of thermal expansion	1/deg C
F	Dimensionless frequency	-
f	Frequency	Hz
L	Length	in
p	Pressure	lbf/in ²
Q	Time constant	1/sec
Re	Reynolds number based on length	-
T	Temperature	deg C
t	Time	sec
u	Instantaneous velocity in x-direction . . .	ft/sec
u'	Velocity fluctuation in x-direction . . .	ft/sec
U	Mean velocity in x-direction	ft/sec
U_∞	Mean free stream velocity	ft/sec
U_0	Mean velocity outside boundary layer . . .	ft/sec
v	Instantaneous velocity in y-direction . . .	ft/sec
x	Distance from leading edge	in
y	Height above flat plate surface	in
δ	Boundary layer thickness	in
δ^*	Boundary layer displacement thickness . . .	in
θ	Temperature difference	deg C
μ	Absolute viscosity	lbf-sec/ft ²
ν	Kinematic viscosity	ft ² /sec
ρ	Density	slug/ft ³
τ	Tension	lbf

Abstract

Wind tunnel experiments were conducted to generate velocity perturbations in a laminar boundary layer using periodic heating of a flush-mounted ribbon. A thin strip of Nichrome ribbon, flush-mounted on a flat plate, was heated by pulsed voltage of various frequencies with spring tension used to take up the slack caused by thermal expansion. Vibration of the ribbon was excited by the periodic thermal expansion and contraction due to the pulsed voltage. Sinusoidal velocity fluctuations were detected by a hot wire anemometer when the ribbon was allowed to vibrate during pulsed heating.

No effect on the amplitude of the flow disturbances was detected with the spring tension removed and segments of the ribbon firmly fixed to the surface such that no vibration of the ribbon occurred during periodic heating. Pulsed heating of a thin ribbon caused detectable flow disturbances only when the ribbon was allowed to vibrate.

The AFIT 9-in wind tunnel had sufficiently low turbulence to detect fluctuations when pulsed voltage was applied to the ribbon. Experiments conducted in the AFIT 14-in wind tunnel were not able to show effects of heating because of the large amount of free-stream turbulence.

BOUNDARY LAYER DISTURBANCES CAUSED BY
PERIODIC HEATING OF A THIN RIBBON

I. Introduction

This thesis examines the generation of periodic velocity disturbances in a laminar boundary layer using periodic heating of a thin ribbon. Such disturbances can be used as a mechanism for the active control of laminar-turbulent transition (9:8). In previous research, disturbances have been generated by vibrating ribbons (11) and by periodic surface heating (7). The present interest in these methods is for the control of flow disturbances using active feedback systems. Instead of changing the mean flow conditions, as is done with suction and blowing boundary layer control schemes, this area of research is aimed at controlling the generation and growth of the disturbances that are predicted by (10) to lead to transition. Disturbances in a laminar boundary layer can be reduced by superimposing control disturbances of the proper phase and amplitude (11).

Background

In a laminar boundary layer, periodic disturbances known as Tollmein-Schlichting (TS) waves develop as a

natural result of surface roughness or perturbations in the external flow (12:382) . A laminar boundary layer is considered stable if the TS waves decrease in amplitude as they move downstream, and unstable if they increase in amplitude. As the TS waves grow in amplitude, some research indicates that they eventually result in turbulent flow (13:69), or they interact with three-dimensional disturbances from the free-stream, causing transition (11:234).

Experiments by Shubauer and Skramstad showed that mechanical oscillations of thin ribbons near a surface generated TS waves and that TS waves at certain frequencies were amplified as predicted by Tollmein-Schlichting theory (13:69-78). However, to reduce the inertia of the ribbon, its thickness was reduced to the point where it was very fragile. It also disturbed the flow when not in use. "Flush-mounted surface heaters have the advantages of being more versatile, less fragile, do not disturb the flow at zero amplitude, and can handle higher frequencies," according to Liepmann (6:187).

Experiments by Liepmann and Nosenchuck (6:187-200) with periodic heating of surface strips in water showed that periodic heating could be used to excite laminar instability waves. The frequency of the unstable waves was typically 40 Hz. Typical heater power was 15 Watts, and the estimated temperature rise was 3C. A second

heater was used to generate a disturbance phase shifted from the first to cancel the first TS wave. When the second disturbance was in phase with the first, the TS wave was amplified. The authors (6:188) hypothesized that with detection of naturally occurring TS waves and an appropriate feedback system, control of naturally occurring TS waves would be possible.

Subsequent research by Liepmann and Nosenchuck (7:201-204), also in water, used a feedback loop with periodic surface heating to reduce the amplitude of naturally occurring TS waves. The amplitude of the TS waves was modified by phase control of the signal to the heater. The net result of reducing the amplitude of the TS waves was to delay the transition to turbulent flow. Heat flux is equivalent to an effective normal velocity at the wall, such as that caused by a vibrating ribbon (6:188). In water, the viscosity decreases as temperature increases, so that steady heating has a stabilizing effect on the laminar boundary layer. The opposite effect occurs in air. Also, the local changes in density are more significant in air than in water, and the resulting governing equations are more difficult to analyze (3:1).

Both surface heating and sound were used by Maestrello (9) to experimentally alter the boundary layer in air. The boundary layer was excited by the heater and the subsequent growth of the disturbances was controlled

by sound. The sign of the pressure gradient determined the receptivity of the flow to periodic heating. In the author's words:

"In the region of favorable pressure gradient the flow is highly receptive to surface heating and one can easily trigger small or large amplitude disturbances as well as impart 'instant' transition. This is an important region of the flow and could be utilized to trigger transition to 'augment' maximum lift of an airfoil." (9:8)

Numerical analysis by Bayliss, et al., (3) showed that the use of localized temperature disturbances was an effective technique for reducing the level of growing disturbances in the boundary layer. The study was based on a fourth-order accurate finite-difference scheme for solving the two-dimensional compressible Navier-Stokes equations. However, there would be some difficulties involved with using heating to reduce the disturbances in air. Larger temperature disturbances are required to change the viscosity in air equivalent to that in water. Also, for compressible flow, temperature disturbances and pressure gradients are coupled and difficult to analyze (3:1). But, in spite of all this, they concluded that localized temperature disturbances could be an effective technique to reduce the level of growing disturbances in the boundary layer.

Another numerical simulation by Maestrello, et al., showed that the pressure gradient induced by curvature of

the surface significantly enhanced the effectiveness of active control of boundary layer disturbances through time-periodic surface heating and cooling (8:5).

Further simulation by Bayliss, et al., (2) of the growth and distortion of disturbances indicated that phase cancellation through active heating and cooling is theoretically feasible. They provided a numerical solution for boundary layer flow with a time harmonic inflow for calculating spatially unstable disturbances. The scheme was applied to study the active control of growing disturbances.

Thomas (11) experimentally used vibrating ribbons in air to actively control boundary layer transition. Transition was successfully delayed, but the flow was not completely restored to its original undisturbed state. Transition was delayed when a second ribbon superimposed phase shifted disturbances of equal amplitude on single-frequency disturbances generated by the first ribbon.

Objective and Scope

The critical element in active boundary layer control is the control mechanism: the method of inducing disturbances in the boundary layer. The objective was to generate and detect disturbances in a laminar boundary

layer using periodic heating of flush-mounted thin ribbons.

Experiments were conducted in two wind tunnels with two different flat plates over ranges of Reynolds numbers from 8000 to 69000, favorable and unfavorable pressure gradients, and 9 configurations. Two methods of attaching the ribbons to the surfaces of the flat plates allowed the ribbons to vibrate mechanically in one case and to be rigidly fixed in the other case, such that only periodic heating would affect the flow. Disturbances of certain frequencies, which vary with Reynolds number, are predicted by Schlichting to lead to transition and therefore are the frequencies that should be generated to control transition. For the range of Reynolds numbers in this thesis, the appropriate frequencies are within the range from 40 to 1000 Hz.

Measurements using a hot wire anemometer gave quantitative data on the amplitude of boundary layer disturbances and qualitative information about the wave forms of the velocity fluctuations.

II. Theory

Disturbances in Laminar Flow

The transition from laminar to turbulent flow begins with the development and growth of periodic velocity perturbations, known as Tollmein-Schlichting (TS) waves. Tollmein-Schlichting stability theory (12:392) says that the growth of the TS waves is governed by the stability of the laminar boundary layer. The stability of the flow is determined by the eigenvalues of the Orr-Sommerfield equation. The result is a relationship between the Reynolds number, the wavelength of the disturbances in the flow, and the stability. Above a critical Reynolds number there exists a range of wavelengths of disturbances for which the laminar flow is unstable. Disturbances of unstable wavelengths will be amplified, while disturbances of larger or smaller wavelengths will be damped out (12:397).

The curves of wave propagation velocity and dimensionless frequency versus Reynolds number for stable and unstable disturbances are given by Schlichting (13:397). The dimensionless frequency is given by:

$$F = \frac{2\pi f}{U_{\infty}} \delta^* \quad (1)$$

where f is the frequency in cycles per second (Hz) and

the boundary layer displacement thickness for a Blasius velocity profile is:

$$\delta^* = 1.72 (\text{Re})^{-1/2} x = 0.344 \delta \quad (2)$$

where Blasius' solution for boundary layer thickness on a flat plate at zero angle of incidence is given by:

$$\delta = 5(\text{Re})^{-1/2} x \quad (3)$$

where $\text{Re} = \rho U_\infty x / \mu$

Equations (1), (2), and (3) with the curves given by Schlichting can be used to determine the frequencies of the unstable disturbances. These are the frequencies of interest that should be controlled to delay transition. Below the critical Reynolds number, finite disturbances can be propagated in the boundary layer, but they will not be amplified until passing downstream of the point where critical Reynolds number occurs.

More detailed theoretical analysis of periodic disturbances in the boundary layer requires sophisticated solution of the Navier-Stokes equations, as done by Bayliss, Maestrello, et al. (2).

A vibrating ribbon at the surface causes velocity disturbances in the boundary layer, as determined by Shubauer and Skramstad (13:75). Periodic surface heating affects the flow in a manner similar to a vibrating ribbon, according to Leipmann (6:188) and Maestrello (9:1). "The coupling between the thermal and mechanical

effects is provided by the dependence of viscosity on temperature," according to Maestrello and Ting (10:1038).

The boundary layer momentum equation given by Liepmann (6:188) indicates the effect of steady surface heating:

$$\rho u \frac{\partial u}{\partial x} + \rho v \frac{\partial u}{\partial y} + \frac{\partial p}{\partial x} - \frac{\partial \mu}{\partial T} \frac{\partial T}{\partial y} \frac{\partial u}{\partial y} = \mu \frac{\partial^2 u}{\partial y^2} \quad (4)$$

In the fourth term on the left side of eq (4), both $(\partial u / \partial y)$ and $(-\partial T / \partial y)$ are positive. In air, $\partial \mu / \partial T$ is positive which is destabilizing (6:188). An increase in surface temperature would cause the right side of the equation to be positive, indicating an inflection in the boundary layer velocity profile, $u(y)$, which Schlichting reports as an indication of an instability (12:390). Also in air, the change in density due to a change in temperature is more significant than in water.

Steady heating of the boundary layer in air has been shown by Nosenchuck, as reported by Maestrello (9:6), to cause transition at lower Reynolds numbers. Periodic temperature fluctuations cause periodic disturbances in the flow. However, the coupling between heating and velocity disturbances in air is much weaker than in water, and is predicted by Maestrello to require a larger temperature fluctuation to cause as large a disturbance in air as in water (9:1).

Temperature Response of Ribbon

A pulsed voltage was applied to the Nichrome ribbon to maximize the amount of fluctuation in temperature. In other research, a sine wave was applied to the heating element, but a sine wave allows less time during which the ribbon could cool, and therefore less fluctuation in temperature. Figure 1 shows the estimated relationship between the pulsed voltage and the temperature of the ribbon.

When voltage was applied, the ribbon heated up and expanded. Between pulses the ribbon cooled and contracted. The periodic expansion and contraction caused the ribbon to vibrate. In the preliminary experiment with the Nichrome ribbon suspended between test stands, as described in section III, the ribbon was seen vibrating during periodic heating.

If gravity is ignored and the displacement is assumed to occur in one plane, then the one-dimensional wave equation can be used to indicate the parameters affecting the frequency of the vibration. The one dimensional wave equation given by Kreyszig (5:417-419) is:

$$\frac{\partial^2 U}{\partial t^2} = c^2 \frac{\partial^2 U}{\partial x^2} \quad (5)$$

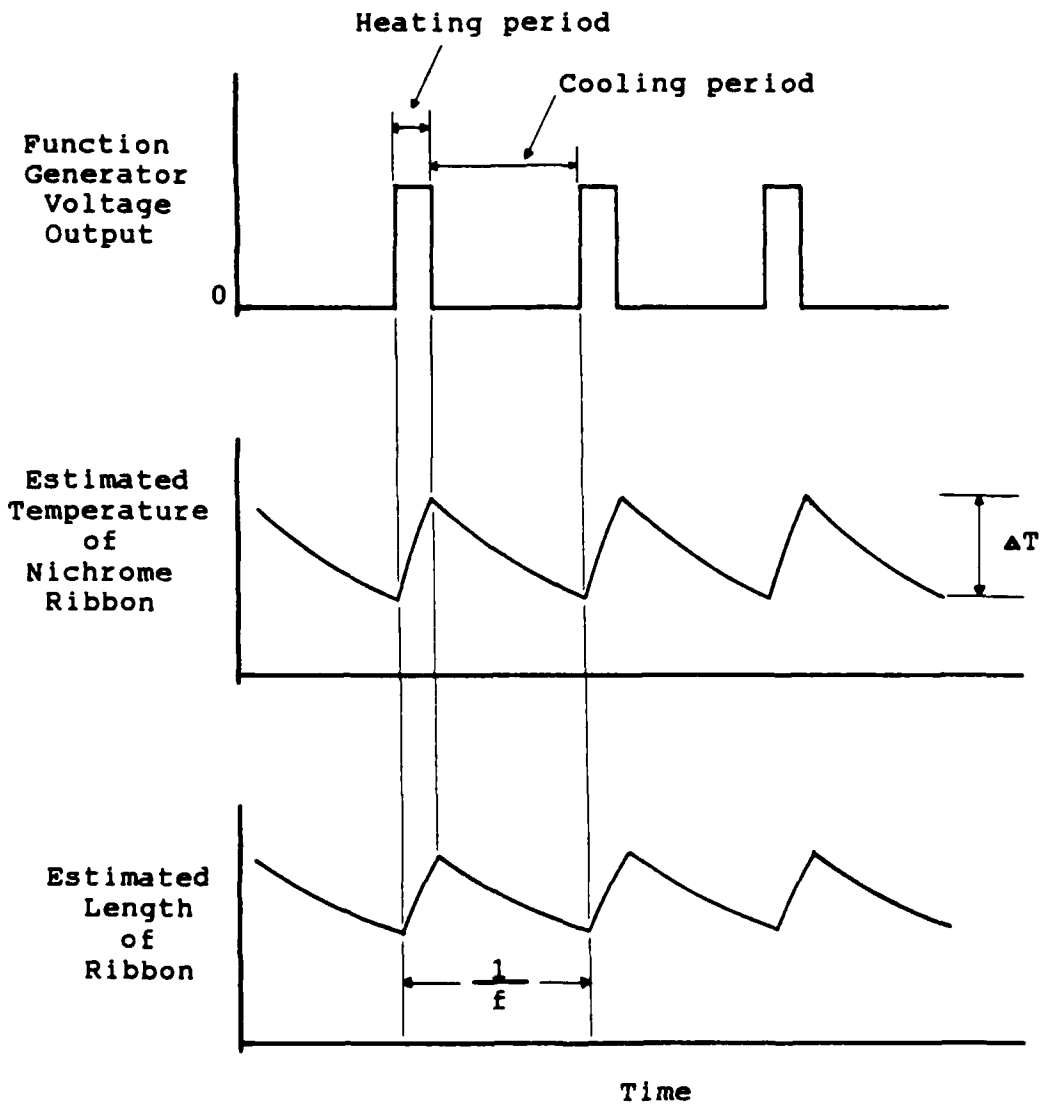


Fig 1. Estimated theoretical response of Nichrome ribbon to pulsed voltage.

where $c = \frac{T}{\rho}$

T is tension, ρ is mass per unit length
and $u(x,t)$ is the displacement.

The solution indicates that the fundamental frequencies of a vibrating ribbon are proportional to the square root of the tension and inversely proportional to the length between fixed end points.

The change in length of the ribbon is proportional to the change in its temperature, assuming a linear relationship exists where the coefficient of thermal expansion is constant. Therefore, the temperature characteristics can be deduced from the thermal expansion properties of the material. The change in length due to thermal expansion is given by:

$$L = L_0 + L_0 C_E (T - T_0) \quad (6)$$

where L is the length when heated to temperature T

L_0 is the length at initial temperature T_0

C_E is the coefficient of thermal expansion

(0.000017 per deg C for Nichrome as given by
the manufacturer)

Solving eq (6) for temperature yields:

$$T = \left[\frac{L}{L_0} - 1 \right] \frac{1}{C_E} + T_0 \quad (7)$$

The temperature fluctuation, ΔT , depends on the amount of time available for cooling between voltage pulses (a function of the frequency, as shown in Fig. 1) and the rate of heat transfer from the ribbon to the air. Convection cooling follows an exponential relationship given by Holman (4:97):

$$\frac{T - T_{\infty}}{T_{\max} - T_{\infty}} = \exp [-(hA/\rho CV)t] \quad (8)$$

which can be rewritten

$$T = T_{\infty} + (T_{\max} - T_{\infty}) \exp [-(hA/\rho CV)t] \quad (9)$$

where T is the temperature of the ribbon as a function of time t , T_{\max} is the initial temperature (heated), T_{∞} is the ambient temperature, C is the specific heat, h is the heat transfer coefficient, A is the surface area of the ribbon, and V is the volume of air into which the heat is transferred. The exponential term $(hA/\rho CV)$ can be considered as a time constant and determined experimentally.

Letting $Q = hA/\rho CV \quad (10)$

$$\theta = T - T_{\infty} \quad (11)$$

$$\theta_{\max} = T_{\max} - T_{\infty} \quad (12)$$

Equation (9) becomes:

$$\theta = \theta_{\max} \exp(-Qt) \quad (13)$$

where Q is a time constant determined by the ability of the ribbon to dissipate heat. The value of Q can be determined experimentally. The change in temperature over time is measured and eq (13) is rewritten as:

$$Q = -\frac{1}{t} \ln(\theta/\theta_{\max}) \quad (14)$$

Equation (7) is used for the length when heated and again for the length at a given time interval after removing steady heat. Then the temperature of the ribbon can be found as a function of time. For pulsed heating, the voltage is applied to the ribbon for 20% of the cycle. The amount of time available for cooling (during which time the temperature decreases as much as it increases during the preceding pulse) is 80% of the period, or $0.8/f$, where f is the frequency of heating. The higher the frequency, the shorter the period, and therefore the smaller the temperature fluctuation ΔT will be. The relationship is:

$$\Delta T = (T_{\max} - T_{\infty})[1 - \exp(-0.8Q/f)] \quad (15)$$

where T_{\max} is the maximum temperature when heated.

Another method was used to estimate the amount of

temperature fluctuation. When pulsed heating was applied, the periodic thermal expansion and contraction of the Nichrome ribbon excited a natural mode and the ribbon vibrated with a displacement normal to the flat face of the ribbon. The maximum and minimum lengths could then be calculated from the measured displacement using trigonometry. Rearranging eq (7) gives an equation for the temperature fluctuation as a function of the maximum and minimum lengths:

$$\Delta T = \left[\frac{L_{\max}}{L_{\min}} - 1 \right] \frac{1}{C_E} \quad (16)$$

Calculations are given in section IV.

III. Experimental Apparatus and Procedure

Apparatus for Preliminary Experiment

The heating element was Nichrome ribbon, 1/16 in wide and 0.002 in thick, approximately the same as that used in previous research by (6), (7), and (9). The ribbon had a resistance of 8 ohms/ft at room temperature.

An experiment was conducted with the heating element suspended between two test stands to determine the response of the heating element to pulsed voltage. The arrangement of equipment is shown in Fig. 2. The airflow over the thin strip of Nichrome ribbon was approximately one foot per second due to the air from the ventilation duct in the lab.

A function generator produced sinusoidal and pulsed voltage output. A Bosen Model 60B Power Amplifier amplified the output of the signal generator. The maximum current was 1.6 amps. A B&K Dual-Trace Oscilloscope measured the voltage output from the signal generator and the power amplifier. A strobe tachometer was used to show the vibrations of the ribbon. The displacement of the ribbon could be measured when the strobe was used to visually freeze the image of the ribbon.

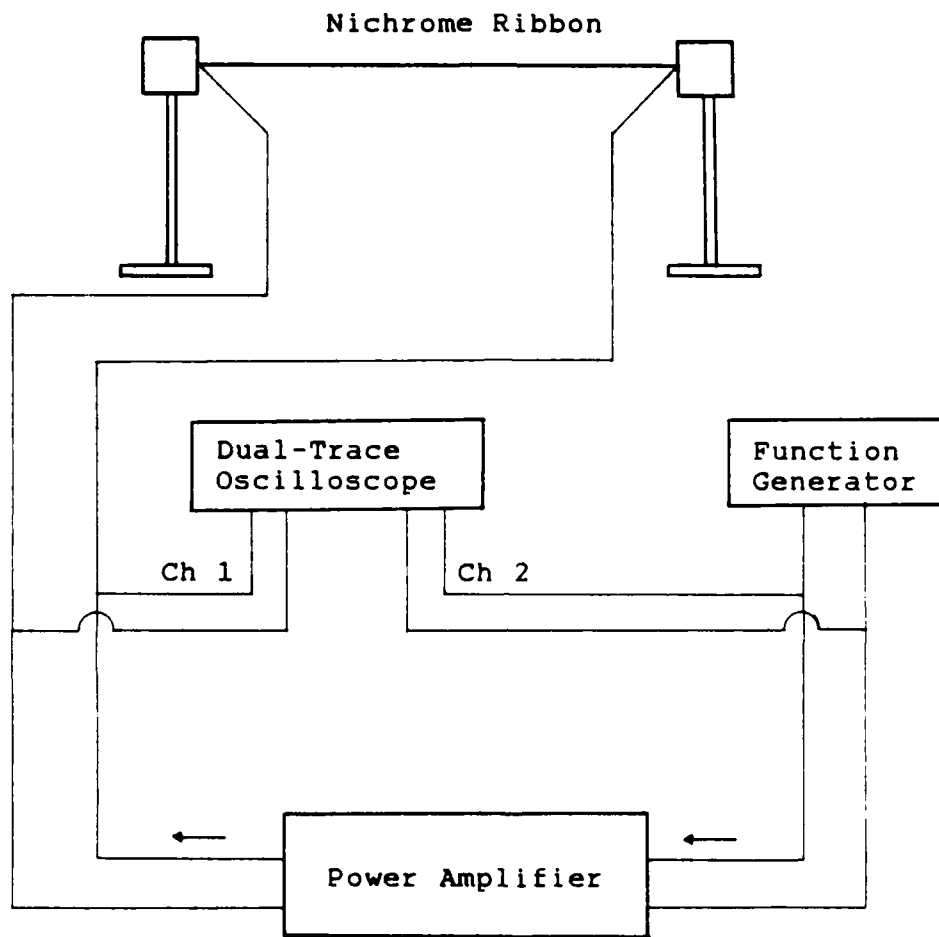


Fig 2. Arrangement of equipment for test of heating element response to pulsed voltage.

Apparatus and Procedure in 14-in Wind Tunnel

The AFIT 14-in wind tunnel is located in building 95A at Wright-Patterson AFB. It is a closed-return type tunnel with a 14-in diameter, 32-in long cylindrical test section. It is powered by a large DC motor and is capable of high subsonic speeds (approximately 600 ft/sec). The arrangement of equipment is shown in Figs 3 and 4. A balance is installed, enabling the incidence angle of the flat plate to be controlled from the console. Pressure measurements were made at different incidence angles to determine the pressure gradient. Velocity and turbulence in the boundary layer were measured with a hot wire anemometer.

The flat plate used in the 14-in tunnel had a 13-in span with a 12-in chord and is shown in Fig 5. It had a rounded leading edge and was made of plexiglass. A one-inch wide strip of phenolic board was embedded three inches from the leading edge, with a shallow groove to hold a Nichrome ribbon heating element. The heating element was held by spring tension to take up slack that occurred as the ribbon expanded during heating. Thirteen ports for sampling the static pressure were located at 1/2 inch intervals along the flat surface of the plate.

The pressure ports were connected by plastic tubing to a Scannivalve, which included a 2.5 psi differential pressure transducer. The signal from the transducer was

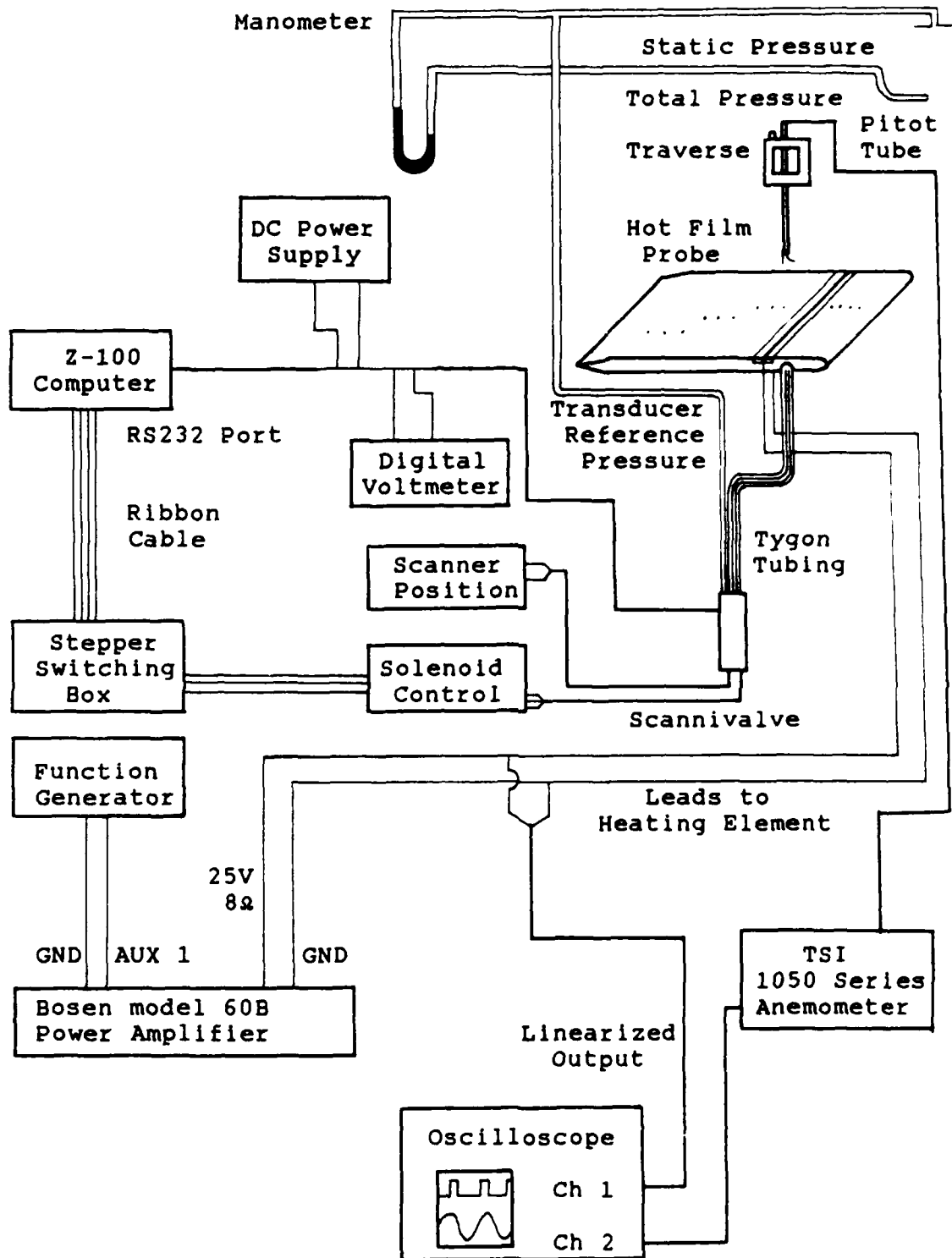


Fig 3. Equipment arrangement at 14-in Wind Tunnel.



Fig 4. Equipment at 14-in Wind Tunnel.

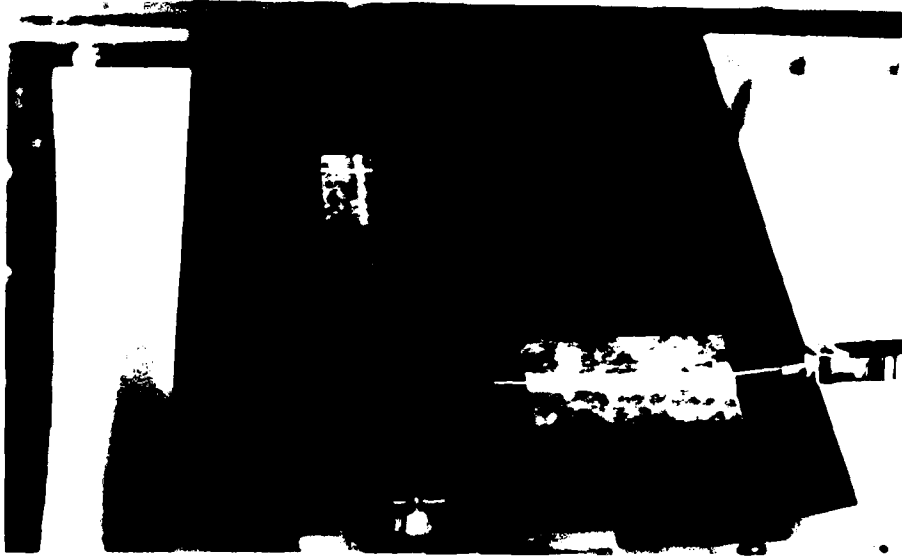


Fig 5. Flat plate in test section of 14-in tunnel.

sent to an AIM-12 Analog-to-Digital (A-to-D) converter card installed in a Zenith Z-100 computer. The AIM-12 was set for a range of -5 to +5 volts with a gain of 100. The Z-100 also commanded the scannivalve to step through the pressure ports. Electromagnetic interference was a problem because the signal from the transducer was so small (-25 to +25 mV full scale). To reduce the noise, the cables between the transducer and computer were shielded and a capacitor was added to the circuit to act as a low-pass filter. The software took N samples and averaged them at each pressure port to reduce the significance of the noise. N was usually 50 to 100 samples. The chordwise static pressure distribution was used to indicate the pressure gradient along the plate.

Velocity and turbulence data were obtained by a Thermal Systems Inc (TSI) 1050 series anemometer. The anemometer output was linear by a linearizing module, then sent to a signal conditioner with a 500 Hz low-pass filter. The output was read from a Hewlett-Packard digital voltmeter. The DC voltage corresponded to the mean flow velocity, and the RMS voltage corresponded to the velocity fluctuations (turbulence).

The TSI 1050 series system is modular with power supply, linearizer, control resistance, and signal conditioner modules. The 500 Hz low-pass filter removed the high frequency interference from the output signal.



Fig 6. Boundary layer Hot Film Probe, TSI Model 1218-20.

The sensor was a TSI 1218-20 hot film boundary layer probe with an operating temperature of 250C, shown in Fig. 6. The probe had a pin to prevent damage to the sensor element by contact with the surface. The pin prevented the sensor from getting closer than 0.005-in from the surface. The sensor was quartz coated platinum alloy 0.002-in in diameter with a 0.04-in long sensing section. The upper frequency response was 250 kHz, according to the manufacturer. The hot film sensor was more durable than a standard hot wire sensor and was less likely to be broken by vibration or flying debris.

The voltage output of the linear anemometer is shown in Fig 7 as a function of velocity. The calibration was accomplished in the 9-in wind tunnel with an empty test section. The velocity was determined by a pitot-static tube connected to an inclined manometer graduated in 0.01-in increments.

The linear output had several advantages over the bridge output, especially when measuring turbulence. The bridge output did not have a straight-line relationship with velocity, therefore the sensitivity was different at each mean velocity and the amount of voltage change for a given velocity fluctuation was a function of the mean velocity. The linear output had a straight-line correlation with velocity. The fluctuation in voltage for a given fluctuation in velocity was independent of the mean velocity, which was important for measuring the distribution of disturbance amplitude across the boundary layer, where there was a significant change in mean velocity.

When the fluid temperature increased, as happened during the heating of the ribbon, the anemometer sensed a decrease in the current required to maintain the sensor at its constant operating temperature. This resulted in a reduction in the indicated mean velocity. However, a given fluctuation in voltage would still correspond to the same fluctuation in velocity, even though the mean

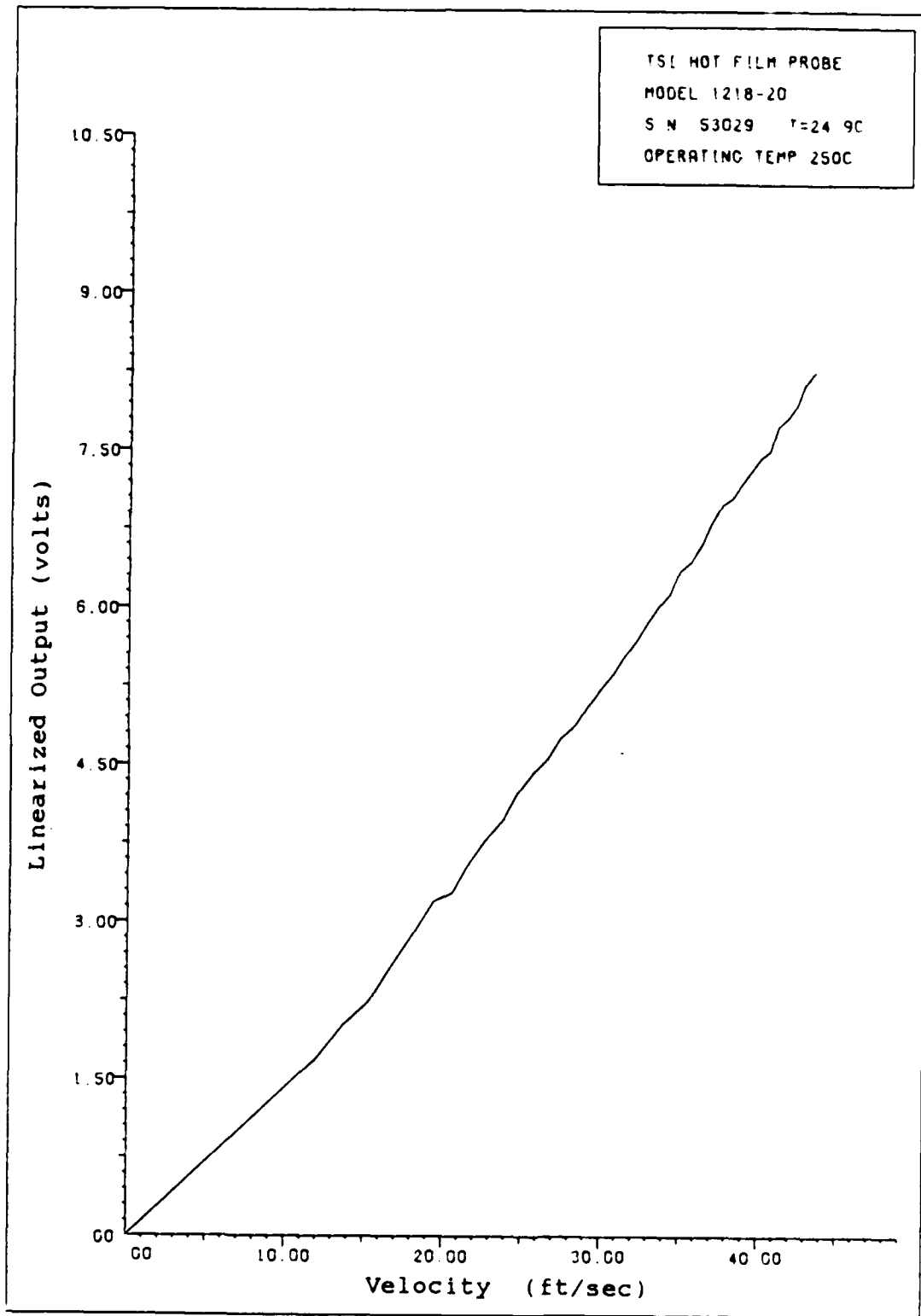


Fig 7. Calibration curve for anemometer output.

indicated velocity would be lower in the heated air. In this way, the measure of turbulence was relatively independent of small changes in air temperature.

Apparatus and Procedure in 9-in Wind Tunnel

The 9-in wind tunnel is located in room 142, building 640. It is an open return type tunnel, designed for low turbulence. Figures 8 and 9 show the general arrangement of equipment. The test section is 9 by 9-in square and 36 in long. The ceiling and floor of the test section are wood and the sides are plexiglass. Test section dynamic pressure was monitored by a two-inch inclined manometer, calibrated in hundredths of inches. The dynamic pressure was measured by the difference between total pressure (ambient static pressure) and the static pressure at four ports (one in each wall) located just upstream of the test section. The DC motor is down stream of the test section and is capable of a maximum velocity of 67 ft/sec in the test section. Free stream turbulence in the empty test section is less than one percent.

The boundary layer hot film probe was mounted in a manual traversing mechanism graduated in 0.001-in increments. The same TSI series 1050 anemometer was used, with linear output and a 500 Hz low-pass filter. The linear output was sent to a digital voltmeter, a storage oscilloscope, and to a modified Z-100 computer.

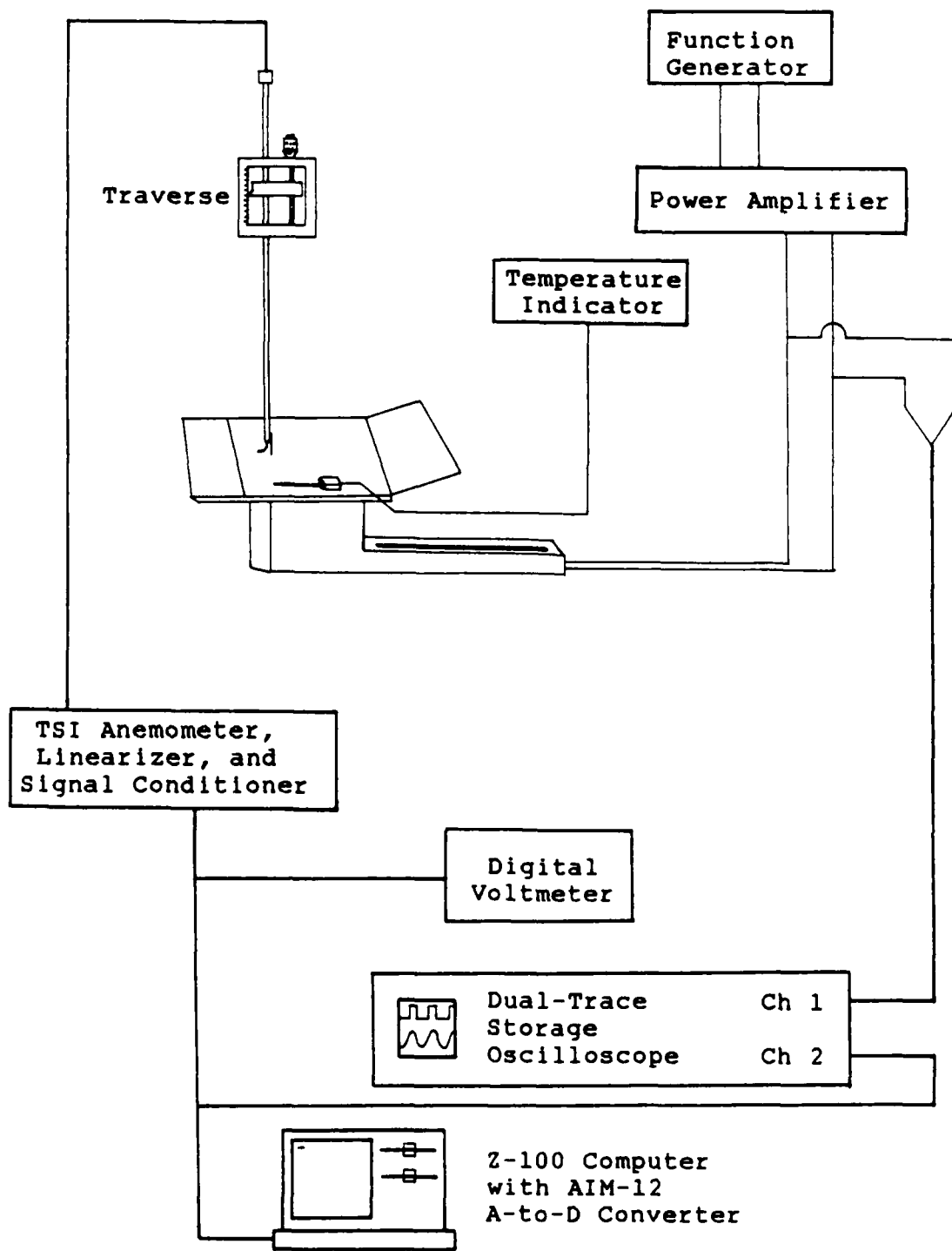


Fig 8. Equipment arrangement at 9-in Wind Tunnel.

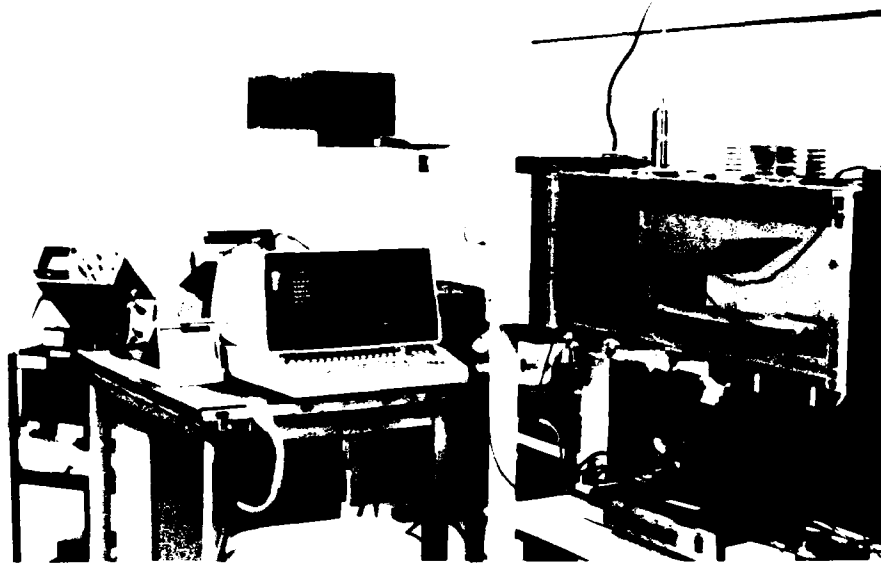


Fig 9. Equipment at 9-in Wind Tunnel.

The computer contained an AIM-12 analog-to-digital converter, set for a range of 0 to 10 volts with a gain of one. The software commanded an A-to-D conversion N times for each data point. From the N sample voltages, a sample mean and sample standard deviation were computed. The computed mean and standard deviation voltages corresponded closely with the digital voltmeter's DC and RMS voltages, respectively (within 1%). The storage oscilloscope displayed the voltage applied to the Nichrome ribbon and the linear anemometer output (velocity fluctuation). Polariod photographs were taken of the oscilloscope presentation to make a permanent record.

The heating element was driven by the same arrangement of a function generator and power amplifier as used in the 14-in tunnel. Fig 10 shows the flat plate mounted in the



Fig 10. Flat plate in test section of 9-in tunnel, with boundary layer hot film probe and temperature sensor.

9-in wind tunnel with the boundary layer probe and temperature sensor. The flat plate model used in the 9-in tunnel was made of a single piece of fiber-reinforced phenolic resin board, 8 by 12 by $\frac{3}{16}$ in. It was mounted on an aluminum support which put the plate in the middle of the test section, and allowed fore and aft adjustment.

With the flat plate alone, separation occurred at the leading edge. Because of the nature of the material, the bevel at the leading edge was not sharp enough to keep the stagnation point on the sharp lip. The velocity and

turbulence profiles at $x=0.5$ in from the leading edge showed that the flow was separated. Farther downstream, the flow reattached, but it was still too turbulent to see any artificially induced disturbances. A flap was added to the trailing edge of the flat plate, deflected upward 30 deg to move the stagnation point up to the lip. With the addition of the flap, the flow was fully attached and laminar. In some experiments, a second heater strip was attached to the plate, electrically in series with the first.

One section of the flat plate that was used in the 14-in tunnel was also used in the 9-in tunnel. It was mounted using a wooden support and had a span of 5.25 in, as shown in Fig 11. Fig 12 shows all the configurations of both flat plates. In configurations 2, 3, and 9 the spring tension was removed and a short (1/2 inch) segment of ribbon directly upstream of the boundary layer probe was fixed to the surface of the plate using adhesive cyanoacrylate (commonly called "super-glue").

Configuration 1 was used only in the 14-in tunnel. A separation bubble at the leading edge of configuration 4 caused the boundary layer to be turbulent. The separation bubble was also present with configuration 6, with a 2-in flap deflected 30 deg. Configuration 5, with a 6-in flap deflected 30 deg, had smooth laminar flow along the entire upper surface. Configurations 7, 8, and 9 had the same

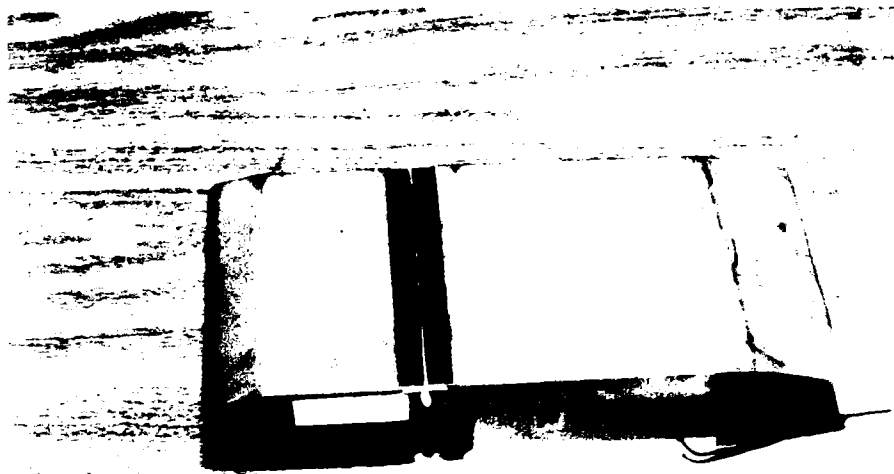


Fig 11. Section of flat plate A for use in 9-in tunnel.

flap arrangement as configuration 5 and differed only in the location of the Nichrome ribbon. Configuration 5 had one ribbon at $x=2$ in. Configuration 7 had 2 ribbons at $x=2$ and $x=3$ in. Configuration 8 had 2 ribbons at $x=1$ and $x=2$ in. Configuration 9 had one ribbon at $x=1$ in.

Static pressure on the plate was not measured directly in the 9-in tunnel, but the sign of the pressure gradient was determined by measuring the velocity at several chordwise locations outside the boundary layer, 2-in from the surface of the flat plate. For example, increasing velocity in the streamwise direction corresponds to decreasing static pressure, indicating a

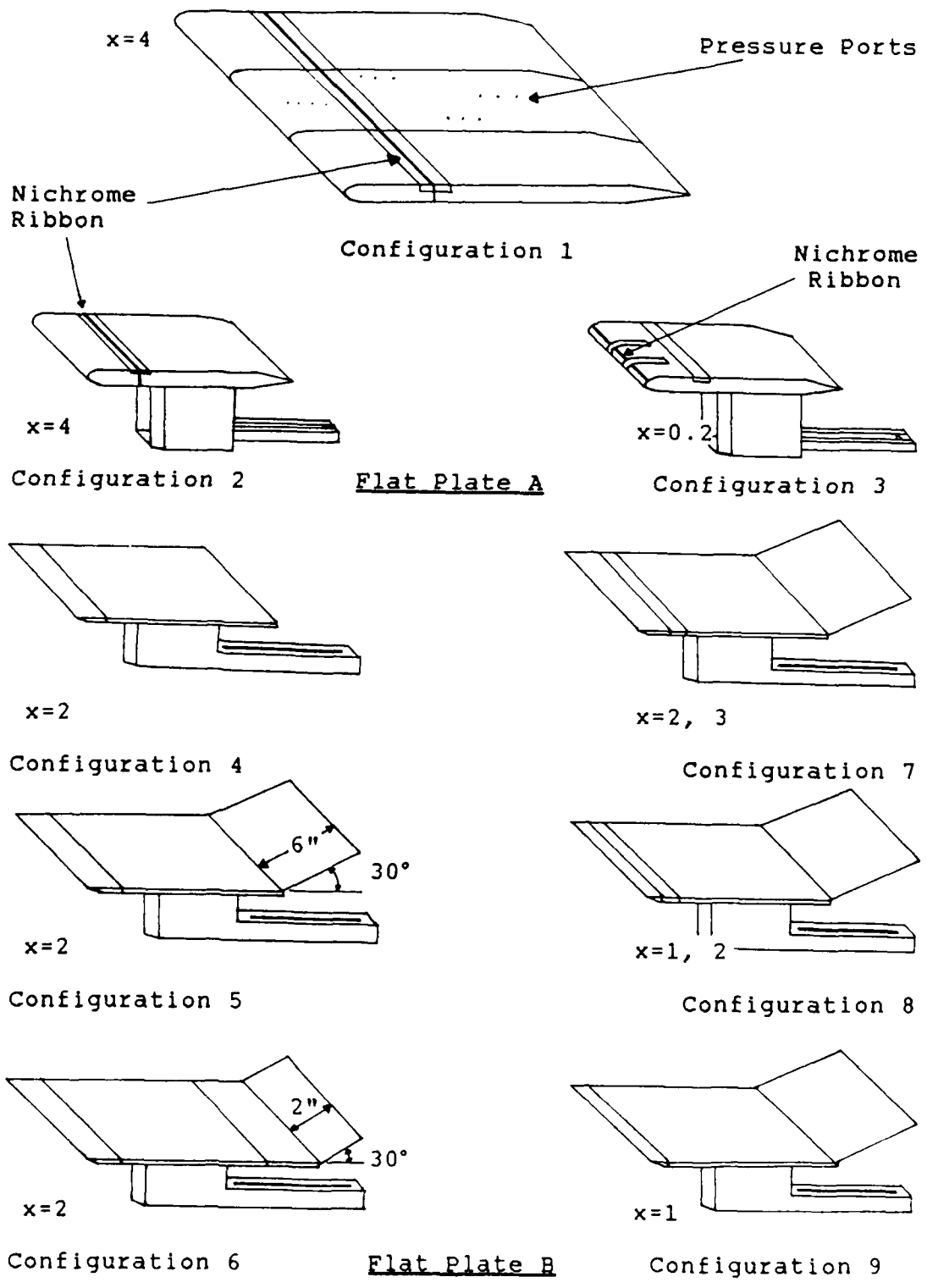


Fig 12. Configurations of flat plates, where x is the location of the ribbon in inches from the leading edge.

favorable pressure gradient.

Vibration of the Nichrome ribbon while mounted on the flat plate was observed with a microscope. A strobe light illuminated the ribbon during pulsed heating. The relative amplitude of the vibrations of the ribbon were measured with markings on the microscope's cross-hair reticle. The displacement due to the vibration was visually compared to the width of the ribbon to estimate the amplitude at various frequencies of pulsed heating.

IV. Results and Discussion

Heating Element Characteristics

The characteristics of the heating element response to pulsed voltage were determined experimentally with the apparatus described in section III (Fig 2) and the equations developed in section II. When voltage was applied to the Nichrome ribbon on the test stand, the ribbon expanded and, at certain frequencies, it vibrated. The vibration was caused by the periodic thermal expansion and contraction as the ribbon was periodically heated and cooled during the voltage cycles.

Using eq (7), the average steady state temperature of the Nichrome ribbon was estimated by measuring the length when heated and comparing it to the length at room temperature. The initial length (L_0) was 11.13 in at a room temperature (T_0) of 22.2C. When the ribbon was heated to the point where it was just beginning to glow red, the length was 11.31 in, with eq (7) giving an estimated temperature of 1013C. When heated by pulsed voltage at 40 Hz, the mean length was 11.22 in, for a temperature of 518C. The accuracy of these estimated temperatures is limited by the assumption that the coefficient of thermal expansion remained constant over a

large temperature range. No other method was used to directly measure the temperature of the ribbon, and therefore the validity of these estimates is not certain.

The rate of cooling was calculated to determine the frequency response using eqs (7), (11), (12), (14), and (15). The length of the ribbon at room temperature, 21C, was 11.09 in. (The length at room temperature was different from the previous paragraph because a different sample of ribbon was used). When heated, the length was 11.25 in, and eq (7) gives a temperature of 850C. The length at one second after turning off electrical power to the ribbon was 11.14 in, and eq (7) gives a temperature of 270C. Substituting the appropriate values into eqs (11), (12), and (14) results in a value for the time constant of $Q = 1.2/\text{sec}$. As an example for pulsed voltage at 70 Hz with $Q = 1.2/\text{sec}$, $T_{\text{max}} = 600\text{C}$, and $T_{\infty} = 21\text{C}$, eq (15) yields a temperature fluctuation of $\Delta T = 8\text{C}$.

Vibration of Ribbon

When pulsed voltage at 35 or 70 Hz was applied to the ribbon on the test stand, the periodic thermal expansion and contraction of the Nichrome ribbon excited a vibration with a displacement normal to the flat face of the ribbon. At other frequencies the amplitude of the displacement was much smaller. A strobe light was used to visually "freeze" the motion of the ribbon to allow the direct

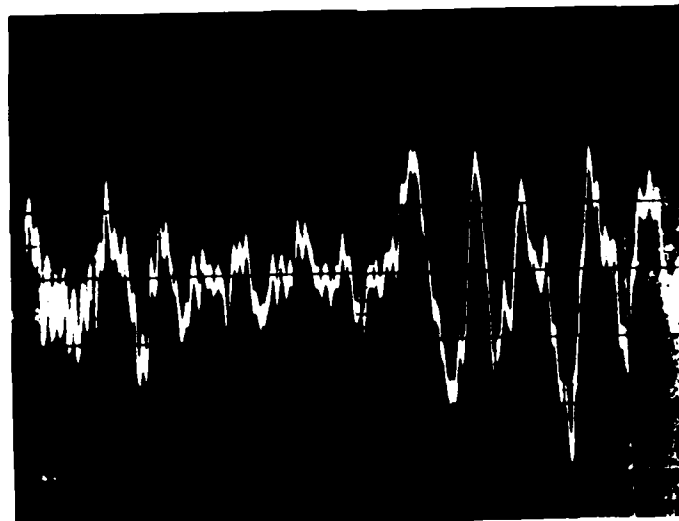
measurement of the displacement. The fluctuation in length was calculated by considering the maximum length to be the hypotenuse of a right triangle with the length at room temperature and the displacement as the two other legs of the triangle. With a measured displacement of 0.19 in, and a minimum length (at room temperature) of 11.125 in, the hypotenuse (maximum length) was 11.127 in. Equation (16) then gives a value for the temperature fluctuation of $\Delta T = 8C$, which is the same as the value computed with eq (15) in the previous paragraph.

With the ribbon held flush against the surface of the flat plate using spring tension (as in configuration 5, Fig 12), the ribbon vibrated during pulsed heating. The amplitude of vibration was observed by using a microscope and a strobe light with the flat plate removed from the wind tunnel, as explained in section III. The amplitude of the vibration was generally on the order of 0.001 inch. At particular frequencies, the amplitude was significantly higher (about 0.005 inch), indicating resonant modes of the ribbon. The largest amplitude occurred when the heating pulses were at approximately 170 and 380 Hz. Increasing the spring tension did not noticeably change the response of the ribbon. Removing all spring tension removed the peak resonant responses but did not completely stop the vibrations.

14-in Wind Tunnel Results

The high level of free stream turbulence in the AFIT 14-in Wind Tunnel prevented the detection of any effect of the heating of the Nichrome ribbons. The screens located upstream of the test section were changed, from two coarse-mesh screens to one coarse-mesh and two fine-mesh screens, but there was no noticeable change in turbulence. Even with the flat plate (configuration 1 in Fig 12) at an angle of incidence to produce a favorable pressure gradient, the free stream turbulence caused the boundary layer to have large random velocity fluctuations.

At an incidence angle of -5 deg (leading edge down) the pressure gradient was favorable, that is, $dp/dx < 0$. An incidence angle of $+5$ deg produced an adverse pressure gradient, $dp/dx > 0$. Figure 13 shows the free stream turbulence detected by the hot film probe. The free stream velocity was 8 ft/sec and the turbulence was 3.6%. Figures 14 and 15 show the boundary layer velocity perturbations without any power applied to the heating element and with periodic voltage applied, respectively. The upper trace is the voltage output of the power amplifier, which was the same as the voltage across the Nichrome ribbon. The lower trace is the AC portion of the linearized anemometer voltage output and indicates the velocity fluctuation in the flow. There was no qualitative or quantitative difference in the boundary



Anemometer
Output
(50 mV/cm)

Time (50 msec/cm)

Fig 13. Free stream turbulence in 14-in tunnel.



Heater
(5 V/cm)

Anemometer
Output
(1 V/cm)

Time (5 msec/cm)

Fig 14. Boundary layer disturbances without heating.
Configuration 1, 14-in tunnel.

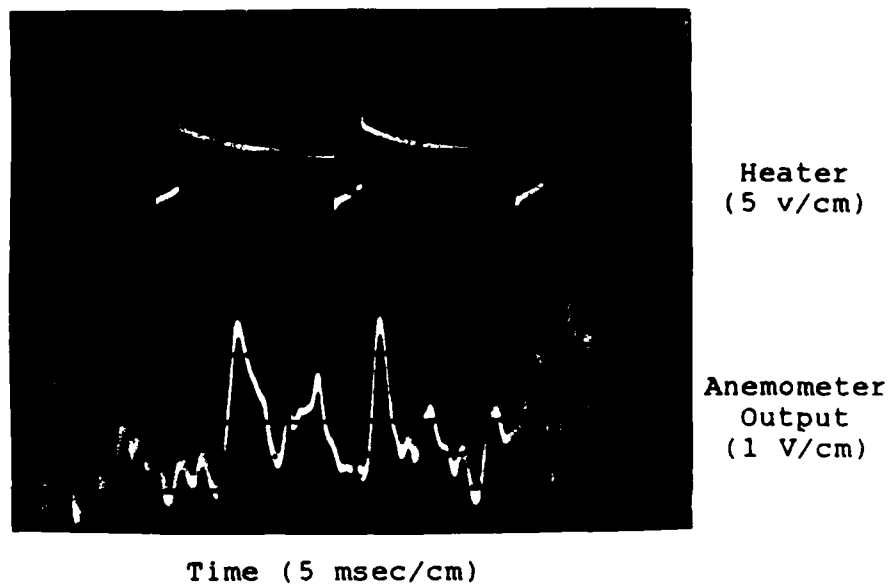


Fig 15. Periodic heating of ribbon in 14-in tunnel.
Pulsed heating at 77 Hz, configuration 1.

layer disturbances between the two cases. The turbulence in both cases was approximately 30%.

9-in Wind Tunnel Results

The AFIT 9-Inch Wind Tunnel had sufficiently low turbulence to permit the detection of velocity perturbations in the boundary layer caused by periodic heating of the ribbon. At certain frequencies of pulsed voltage, the amplitude of velocity perturbations increased dramatically.

With the flat plate configurations 5, 7, 8, and 9, as

shown in Fig 12, the boundary layer was found to be laminar over the entire length. The highest Reynolds number examined was 200,000 per foot. The 30 deg flap at the trailing edge prevented separation at the leading edge, which occurred with configurations 4 and 6.

The pressure gradient along the flat plate was estimated from the mean velocity outside the boundary layer at various distances from the leading edge, as described in section III. The velocity gradually decreased from the value at the leading edge by 4% over the first 4 in aft from the leading edge. A decrease in velocity theoretically corresponds to an increase in static pressure, therefore an adverse pressure gradient was present ($dp/dx > 0$).

Fig 16 is a photograph of the oscilloscope presentation showing the background turbulence level in the laminar boundary layer with no voltage applied to the ribbon. The plate was at zero incidence angle with the trailing edge flap deflected up 30 deg (Configuration 7 in Fig 12). The free stream velocity was 34 fps with a Reynolds number of 69,000 at the hot film sensor, which was located at $x = 4$ in, where the boundary layer thickness was $\delta = 0.081$ in. Nichrome ribbons were located at $x = 2$ in and $x = 3$ in.

With pulsed voltage at 177.5 Hz and the sensor at $y = 0.005$ in above the plate surface, or $y/\delta = 0.06$, Fig 17

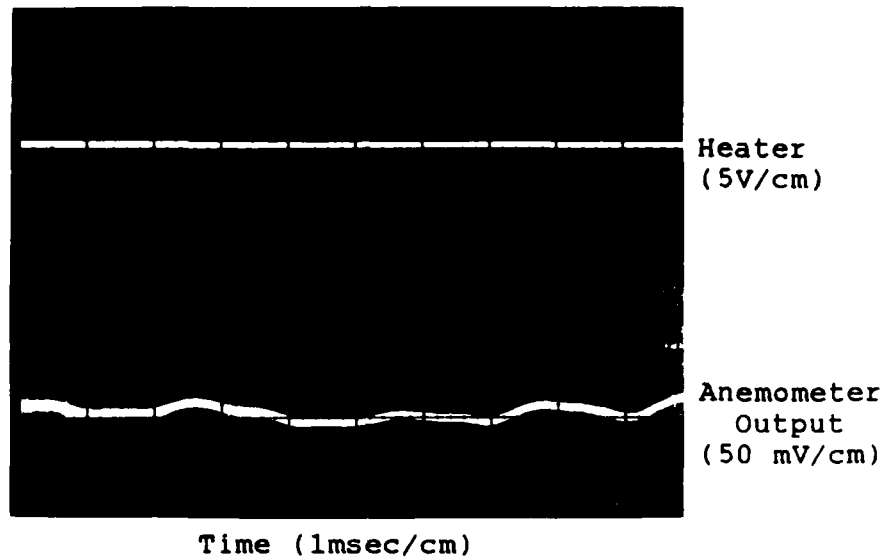


Fig 16. Boundary layer in 9-in tunnel, no heat.
Configuration 7, sensor at $y/\delta = 0.06$.

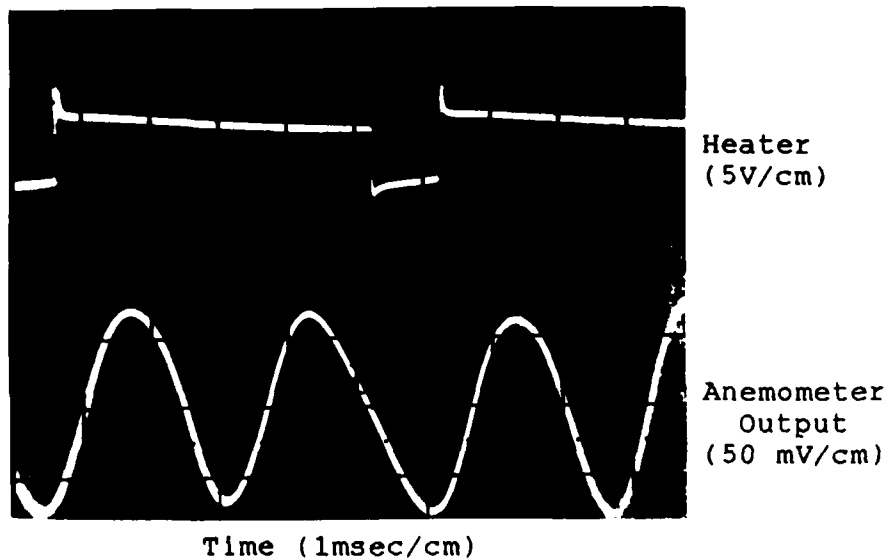


Fig 17. Periodic heating of ribbon, $y = 0.005$ in,
 $y/\delta = 0.06$. Pulsed heating at 177 Hz,
response at 355 Hz. Ribbon vibrating.

shows sinusoidal velocity fluctuations. The sinusoidal velocity fluctuation shown in Fig 17 is representative of all the test results where the ribbon was allowed to vibrate when pulsed voltage was applied. Also, Fig 17 shows that the frequency of the disturbances was twice the frequency of the pulsed voltage across the ribbon, or 355 Hz. Note that the velocity perturbation showed a minimum directly below the pulse.

In Fig 18, at $y = 0.06$ in, or $y/\delta = 0.74$, the amplitude of the disturbance diminished to approximately the level of the naturally occurring free stream turbulence. In Fig 19, at $y = 0.08$ in or $y/\delta = 0.99$, the velocity was at a peak just below the pulse. A 180 degree phase shift occurred, as previously demonstrated by Shubauer and Skramstad (14:76), and also as predicted in the numerical simulation by Bayliss, et al. (2:7). The results shown were typical for conditions where the ribbon was allowed to vibrate.

The dimensionless velocity profile is shown in Fig 20, where the boundary layer thickness was 0.081 in thick. For these conditions, Blasius' theory for a flat plate at zero incidence predicts a boundary layer thickness of 0.076 in. The mean velocity at each point has been non-dimensionalized by the mean velocity (U_o) outside the boundary layer at the same x location. U_o was 4% less than U_∞ , which was measured just upstream of the test section. A straight line connects each data point.



Fig 18. Periodic heating of ribbon, $y = 0.06$ in, $y/\delta = 0.74$. Pulsed heating at 177.5 Hz, ribbon allowed to vibrate.

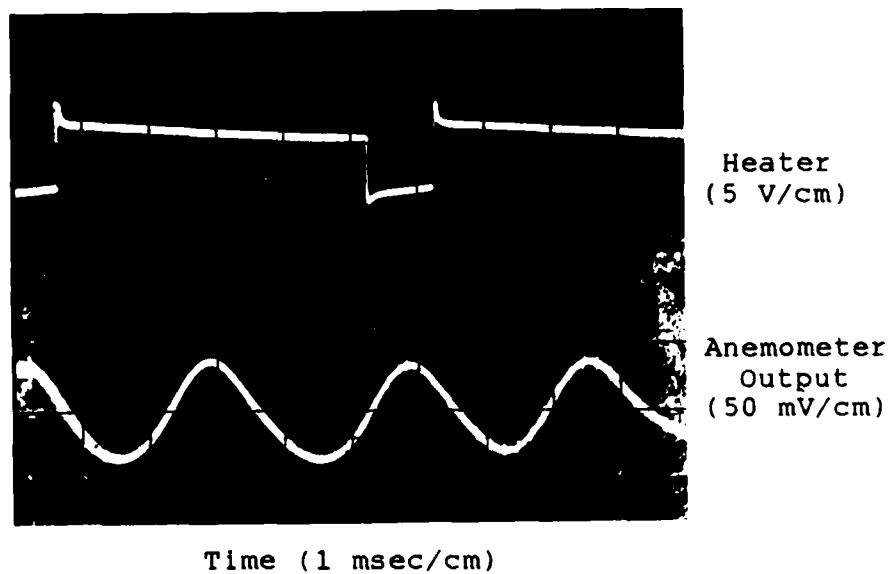


Fig 19. Periodic heating of ribbon, $y = 0.08$ in, $y/\delta = 0.99$. Pulsed heating at 177.5 Hz, response at 355 Hz, vibrating ribbon.

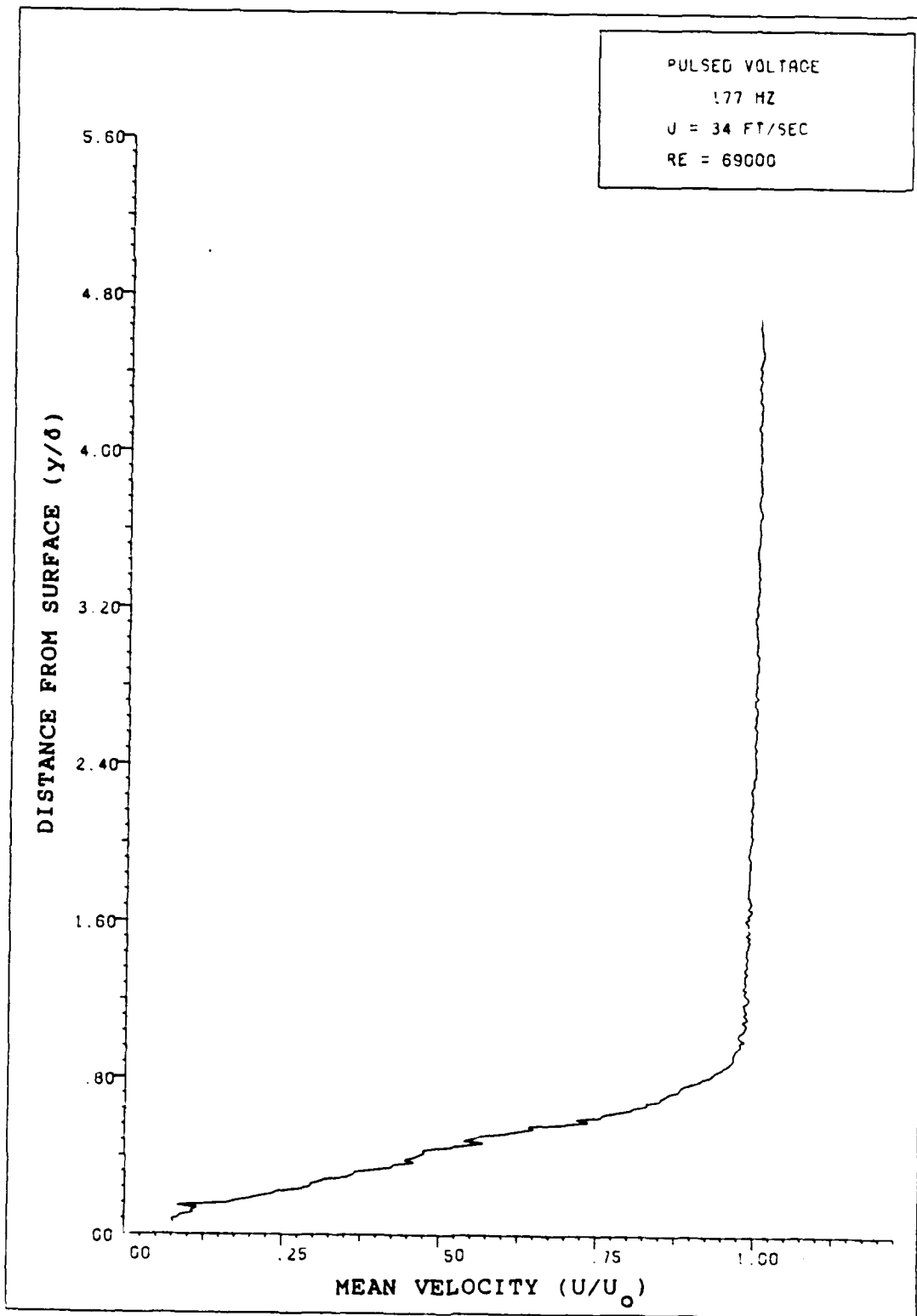


Fig 20. Dimensionless velocity profile.

Figure 21 shows the dimensionless turbulence profile which agrees with the shape found in the experiments by Shubauer and Skramstad with a vibrating ribbon (12:76). The turbulence has been non-dimensionalized by the same mean velocity outside the boundary layer that was used to non-dimensionalize the velocity profile. The distribution of amplitude across the boundary layer shown by Fig 21 also agrees qualitatively with the numerical solution of the Navier-Stokes equations by Bayliss, Maestrello, et al., (3:4) as shown by the dashed line in Fig 21.

Previous experiments with vibrating ribbons used an alternating current and electromagnets located beneath the surface of the flat plate. In the present experiment, there are no magnets, only the pulses of voltage causing rapid thermal expansions and contractions of the ribbon.

Fig 22 shows the distribution of velocity perturbation amplitude against the frequency of the voltage applied to the Nichrome ribbon. A straight line connects each data point. The relative amplitude is the RMS value of the voltage output of the linearized anemometer divided by the RMS value with no voltage applied to the ribbon. However, the frequency of the response of the boundary layer remained at about 350-370 Hz throughout the range of input frequencies, as seen in Fig 17, where the input frequency is 177.5 Hz and the response of the boundary layer is at 355 Hz. When the

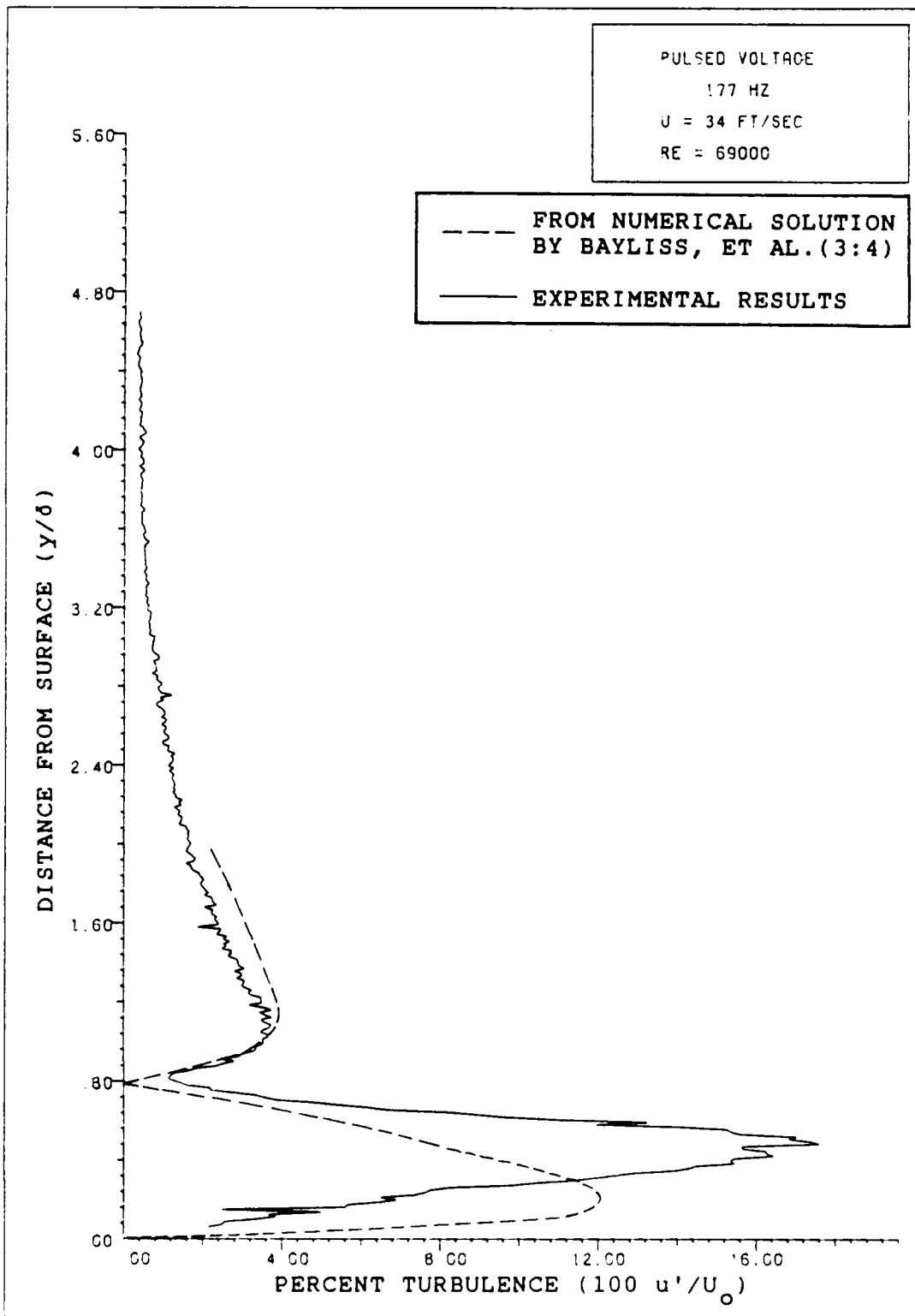


Fig 21. Turbulence profile, vibrating ribbon.

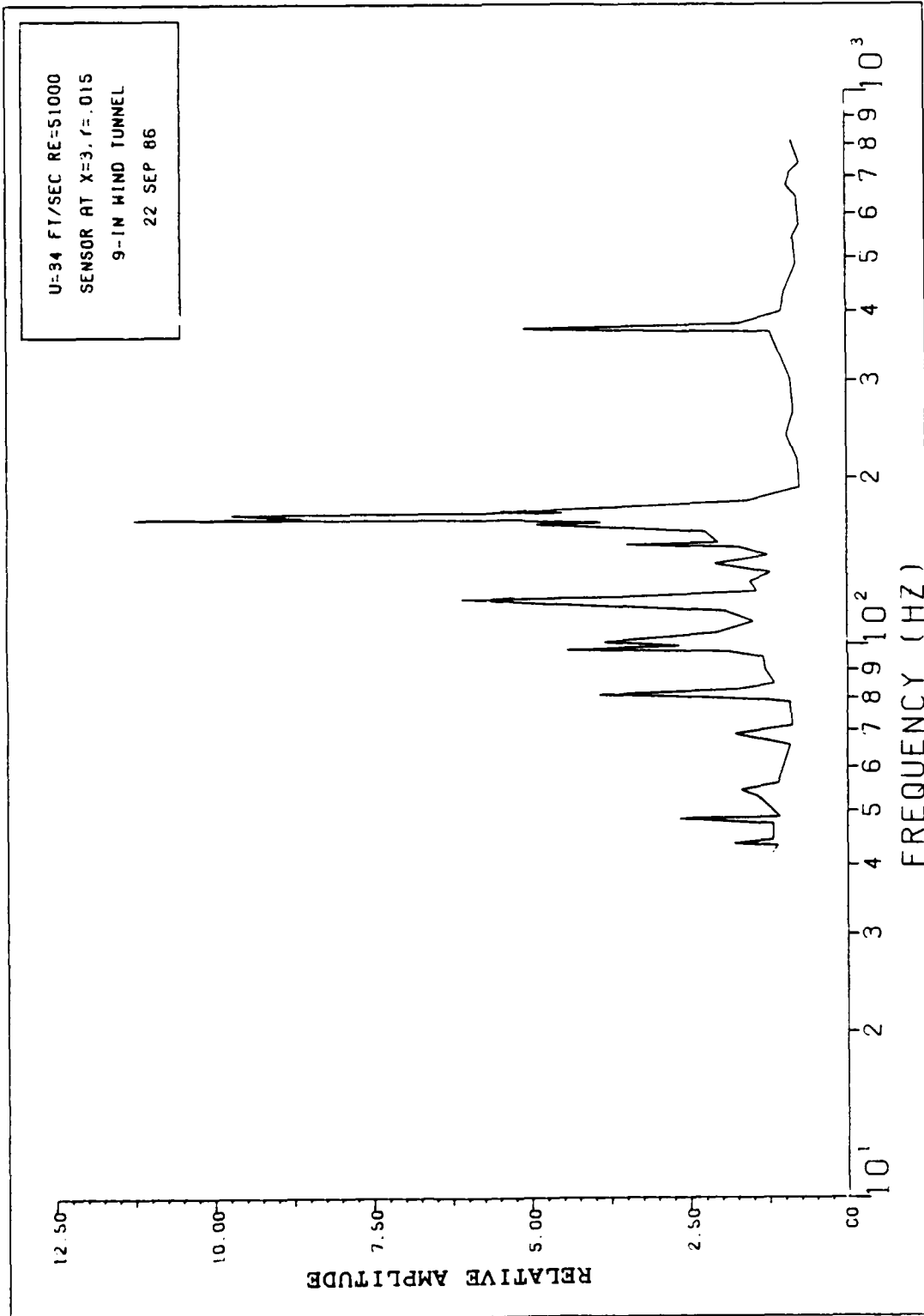


Fig 22. Relative amplitude vs pulse frequency. Frequency of response was 350-370 Hz.

input frequency was 371 Hz (the highest frequency peak in Fig 22), the boundary layer response was also 371 Hz.

The peaks in Fig 22 seem to correspond to the peaks in amplitude of vibration of the ribbon which were seen when the ribbon was examined under a microscope with a strobe light, using the procedure described in section III. Under the microscope with the flat plate removed from the wind tunnel, the largest amplitudes of vibration of the ribbon were seen when the voltage pulses were at approximately the same frequencies as the peaks in Fig 22.

Alternative Causes of Velocity Fluctuations

Some other possible causes of the observed phenomena are electromagnetic interference, acoustic noise induced disturbances, vibration of the flat plate, vibration of the hot film probe support, or thermal effects due to the heating of the ribbon.

The first phenomena to suspect is electromagnetic or radio frequency (RF) interference. Sources of possible RF interference are the 60 Hz AC line current throughout the building, RF noise from the DC wind tunnel drive motor, located approximately 10 ft from the test section, and RF noise due to the pulsed voltage in the heater strip. With no voltage applied to the heater strip, and even with the tunnel motor running and flow through the test section, no regular disturbances appeared. Fig 17 shows the response

of the flow to periodic heating of the ribbon. By comparison, Fig 16, without heating, shows the low level naturally occurring disturbances. In both figures the environment is the same, except for the voltage applied to the ribbon. Causes other than those related to the heating element system can be eliminated because there were no similar responses without voltage applied to the ribbon. This means that the tunnel drive motor, AC line current, and tunnel acoustic characteristics can be ruled out as causes of the disturbances seen in Fig 17.

It is logical to expect that the alternating current applied to the heater strip would induce a voltage in the hot film probe, since both are parallel to each other. This means that the hot film probe would be acting like a radio antenna. Because of the short length of the sensor, it is most sensitive to short wavelength signals of higher frequencies than those used in the boundary layer experiments. Indeed, Fig 23 shows small disturbances coinciding with the voltage pulses even with no flow and therefore no mechanical connection between the ribbon and the probe. The anemometer output amplitude scale in Fig 23 is 20 mV/cm, much smaller than the scale in Fig 17, 50 mV/cm. Therefore the RF-induced disturbances are smaller and of a shape that is noticeably different from the wave form of the velocity perturbations associated with the periodic heating of the ribbon.

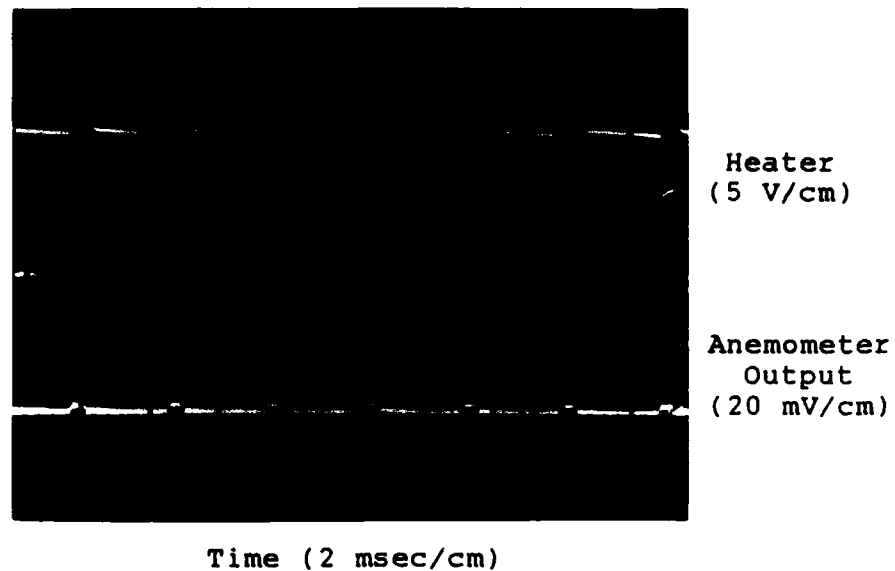


Fig 23. Anemometer response with no flow.

Heating Without Vibration

A section of the ribbon was securely fixed to the to the surface to determine effects on the boundary layer due to periodic heating without mechanical vibrations (Configurations 3 and 9 from Fig 12). When examined under the microscope with a strobe light during periodic heating the ribbon segment did not show any movement in any direction.

With the plate and fixed ribbon in the wind tunnel, the boundary layer was examined for indications of

velocity disturbances due to periodic heating. The velocity of the tunnel was varied from 5 to 35 ft/sec, the heating pulses were varied from 40 to 1000 Hz, and the ribbon was moved to various locations on both flat plate models (Configurations 2, 3, and 9 in Fig 12) with neutral, slightly favorable, and strongly favorable pressure gradients. In all cases, there was no indication of any qualitative or quantitative change in the boundary layer velocity characteristics.

A comparison of the hot film probe output without and with heating is shown in Figs 24 and 25, respectively. The small disturbances visible in Fig 25 directly beneath each heat pulse were caused by electromagnetic influence and do not indicate a phenomena related to the flow. This is shown in Fig 23, when the same heating was applied with no flow.

The distribution of turbulence with height above the flat plate is shown in Fig 26 with no heat and in Fig 27 with pulsed heat at 352 Hz. It can be seen that there was no difference in amplitude.

The mean velocity profiles, Fig 28 (no heat), and Fig 29 (pulsed heat), show a decrease in velocity with heating but this is explained as an error due to the change in temperature of the boundary layer. The boundary layer temperature increased about 10C with the heat on, and this temperature increase caused a reduction in the rate of

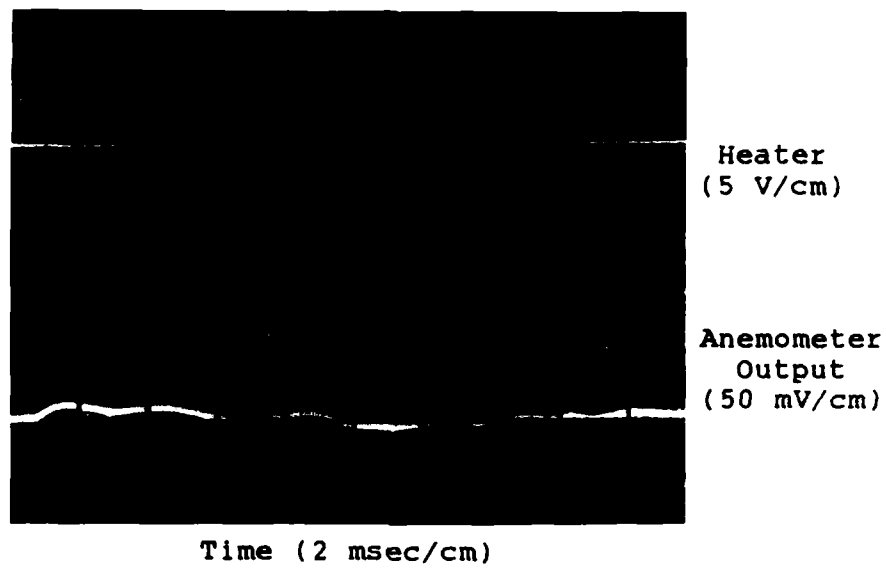


Fig 24. Boundary layer, no heat. Configuration 3, ribbon not allowed to vibrate.

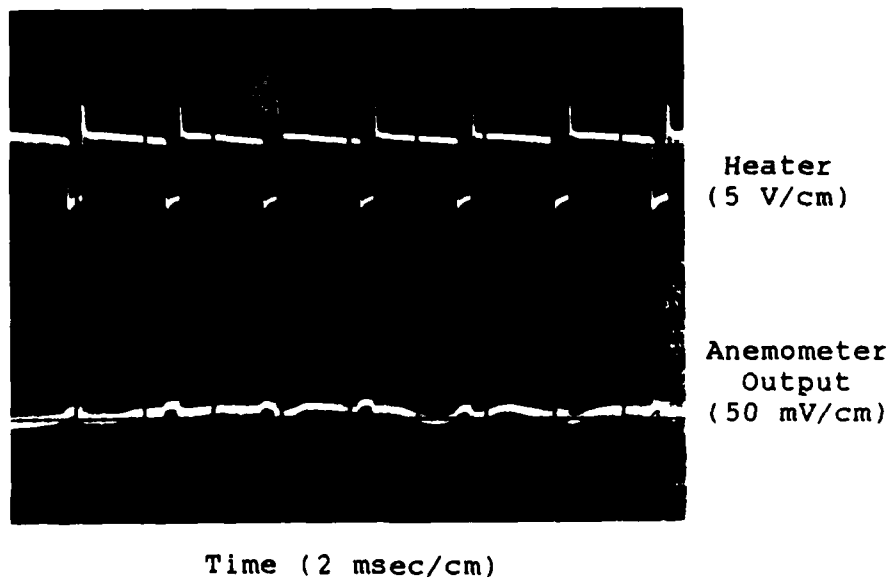


Fig 25. Periodic heating of non-vibrating ribbon. Configuration 3, ribbon not allowed to vibrate.

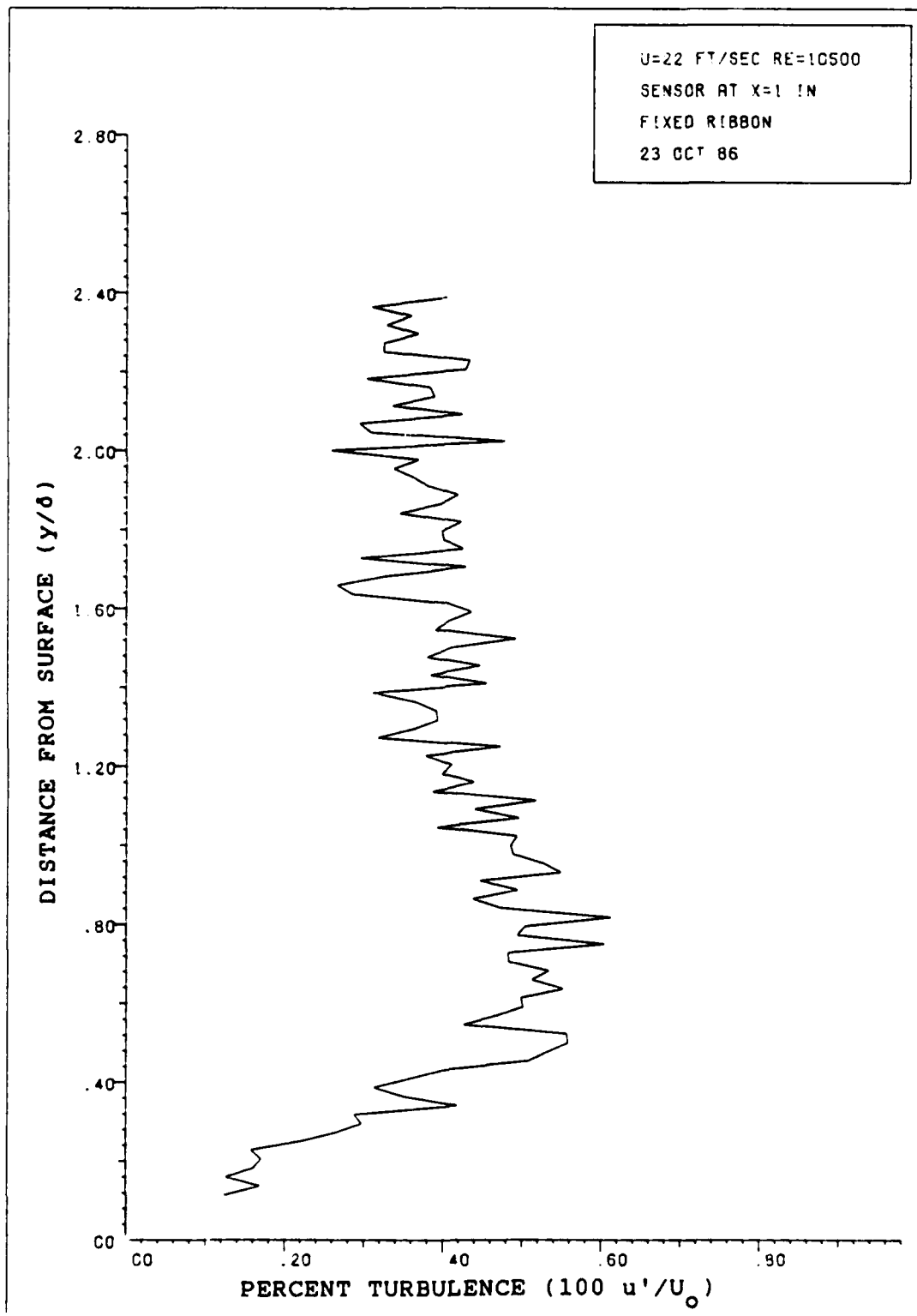


Fig 26. Turbulence profile, no heat.

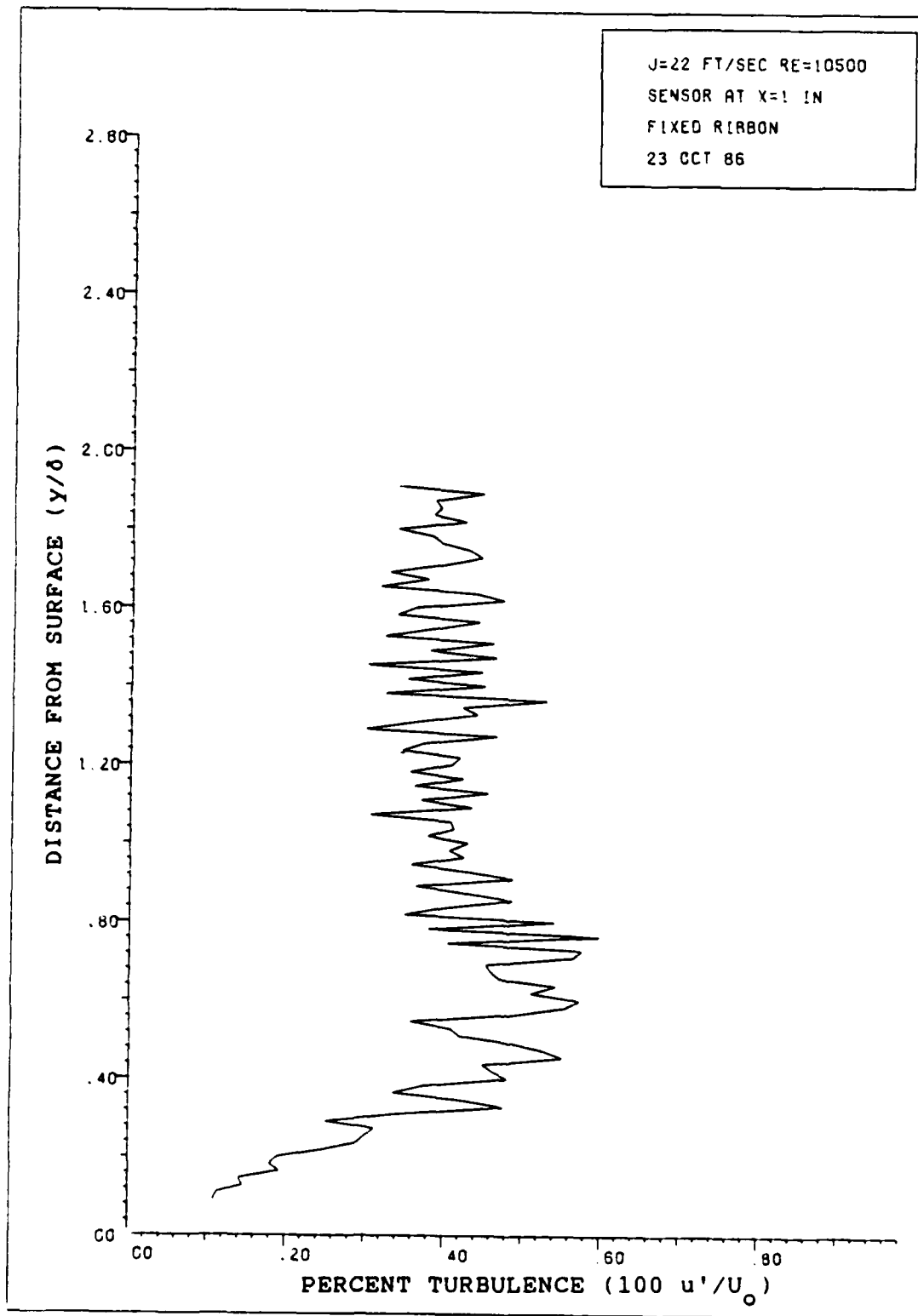


Fig 27. Turbulence profile, pulsed heat.

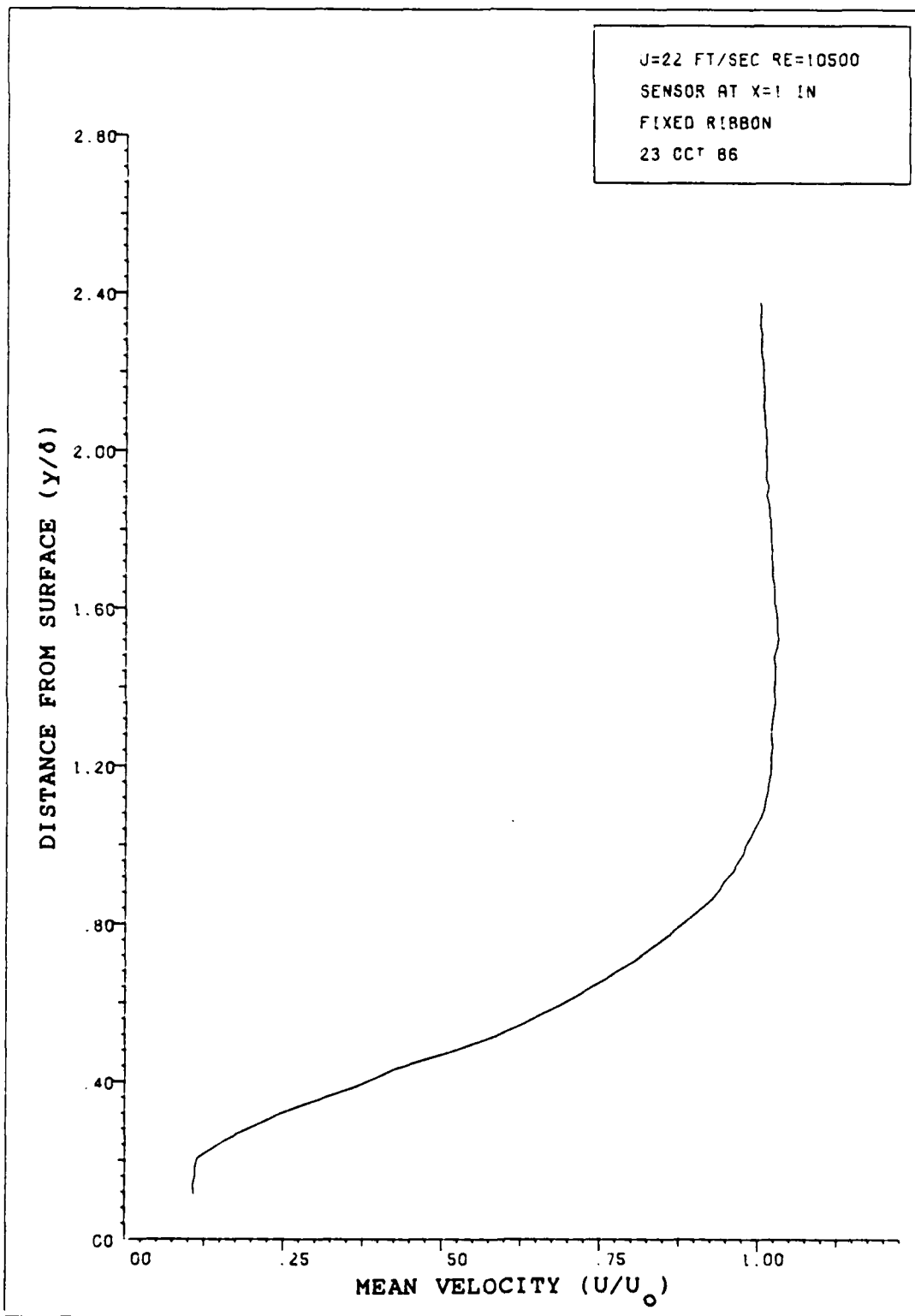


Fig 28. Dimensionless velocity profile, no heat.

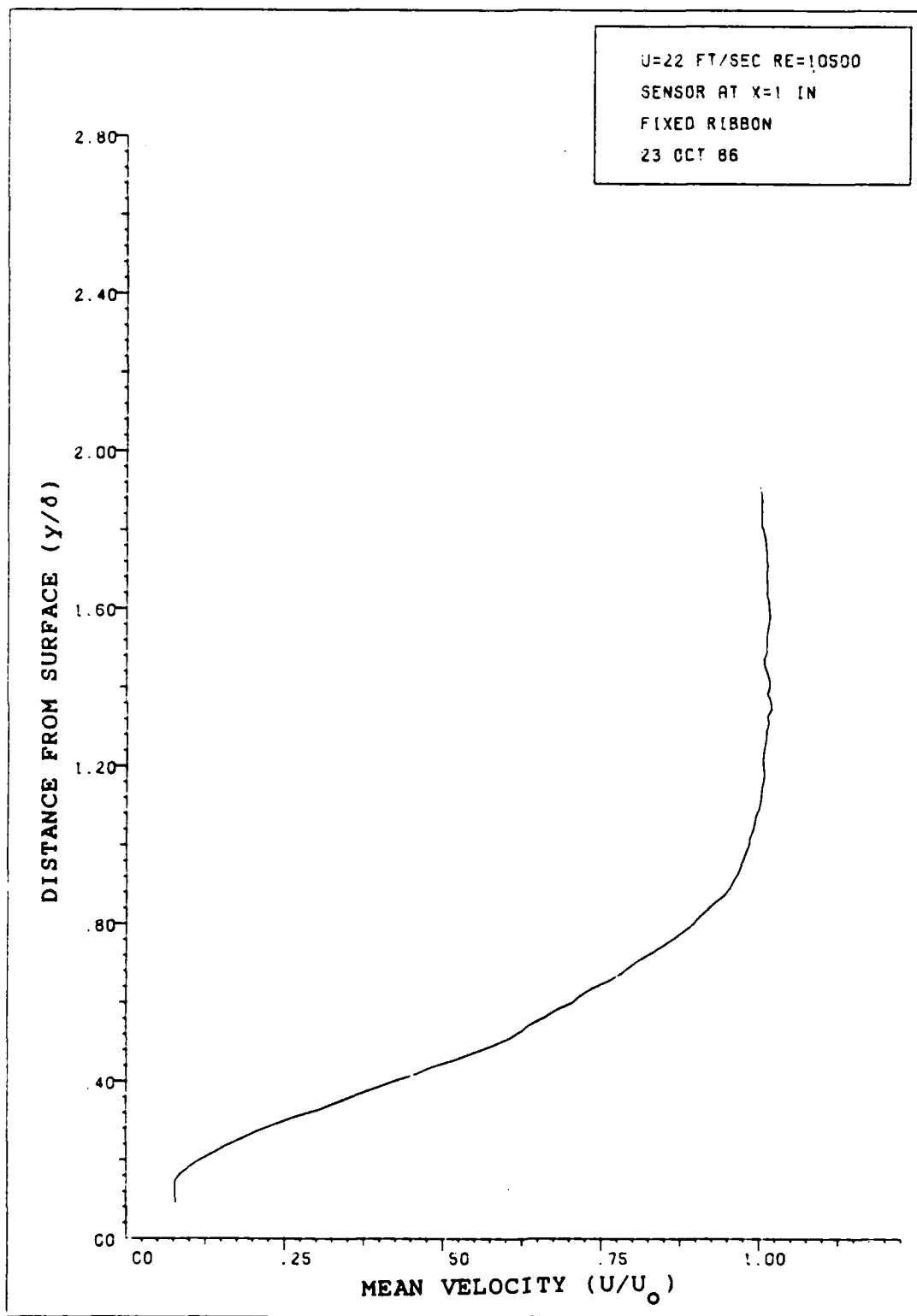


Fig 29. Dimensionless velocity, pulsed heat.

heat transfer away from the hot film sensor. The anemometer constant temperature circuit then reduced the amount of current needed to maintain the probe at its constant temperature. Therefore the voltage output from the anemometer was reduced even though the velocity of the flow may not have changed.

While it seems clear that vibration of the ribbon caused the observed sinusoidal velocity fluctuations, the possible effects of the pulsed heating, which accompanied the vibration (and in fact caused the vibration), cannot be ruled out. The heat transfer characteristics of the heating element system may have been altered by gluing the ribbon to the surface. The firm contact could have caused an increase in conduction heat transfer into the substrate, decreasing the effective heat transfer to the boundary layer.

V. Conclusions and Recommendations

Conclusions

The results of this research indicate the following conclusions:

1. Pulsed voltage applied to a thin Nichrome ribbon that was free to move caused vibration by rapid thermal expansion and contraction at frequencies and amplitudes that could be useful for active boundary layer control.

2. The periodic heating of a fixed, non-vibrating ribbon did not cause detectable disturbances in the boundary layer for the flow conditions examined. However, the method used to fix the ribbon to the surface may have altered the heat transfer characteristics. Therefore the velocity fluctuations observed when the ribbon vibrated may also have been influenced by the heating.

3. The method of vibrating a flush-mounted ribbon by pulsed voltage is at least as effective as Shubauer and Skramstad's (14) method of using electromagnets with a thin ribbon placed a short distance away from the surface.

4. The flush-mounted ribbon did not appreciably disturb the flow when no voltage was applied.

Recommendations

Additional research could further investigate the characteristics of periodic heating of a thin ribbon and its effects on the boundary layer. Some additional equipment is recommended to conduct further research:

A longer flat plate with a rounded leading edge and a moveable flap would be useful for investigating transition and the amplification and damping of disturbances.

High speed photography of the vibrating ribbon could be used to more accurately determine the frequency and amplitude of the vibrations.

A temperature-compensated hot wire anemometer probe could be used to determine the effects of heating on the mean velocity profile, $U(y)$. In the present study the changes in the mean velocity could not be distinguished from the effect of changing air temperature.

Multiple hot wire/film anemometer probes and support systems are necessary to examine the downstream propagation of disturbances. Comparison between upstream and downstream sensors would indicate the growth or decay of artificially induced velocity fluctuations. Also, a spectrum analyzer would be beneficial in determining the frequency distribution of disturbances in the flow.

The ability of the periodic surface heating without vibration to generate disturbances of finite amplitude in air could be improved by a more powerful amplifier and by

more responsive heating elements. The ideal heating element would have very low thermal inertia to respond rapidly to pulsed voltage, resulting in greater fluctuation in temperature. It must also be rigidly mounted in a way that prevents vibration of the element, in order to distinguish between the effects of heating and the effects of vibration.

A feedback control system for actively controlling laminar boundary layer disturbances could be developed using flush-mounted, thermally-pulsed vibrating ribbons.

Bibliography

1. Bayliss, A., L. Maestrello, P. Parikh, and E. Turkel. "Wave Phenomena in a High Reynolds Number Compressible Boundary Layer," Contract numbers NAS1-17070, NAS1-18107. Institute for Computer Applications in Science and Engineering, NASA Langley Research Center, Hampton, VA, November 1985 (N86-19554).
2. Bayliss, A., P. Parikh, L. Maestrello, and E. Turkel. "A Fourth-Order Scheme for the Unsteady Navier-Stokes Equations," AIAA 18th Fluid Dynamics and Plasmadynamics and Lasers Conference. Paper No. 85-1694, American Institute of Aeronautics and Astronautics, New York, July 1985.
3. Bayliss, A., L. Maestrello, P. Parikh, and E. Turkel. "Numerical Simulation of Boundary Layer Excitation by Surface Heating/Cooling," AIAA Shear Flow Control Conference. Paper No. 85-0565, American Institute of Aeronautics and Astronautics, New York, March 1985.
4. Holman, J.P. Heat Transfer. (Fourth Edition). New York: McGraw-Hill Book Co., 1976.
5. Kreyszig, E. Advanced Engineering Mathematics. (Third Edition). New York: John Wiley and Sons, Inc., 1972.
6. Liepmann, H.W., G. L. Brown, and D. M. Nosenchuck. "Control of Laminar Instability Waves Using a New Technique," Journal of Fluid Mechanics, 118:187-200 (1982).
7. Liepmann, H.W. and D. M. Nosenchuck. "Active Control of Laminar-Turbulent Transition," Journal of Fluid Mechanics, 118: 201-204 (1982).
8. Maestrello, L., A. Bayliss, P. Parikh, and E. Turkel. "Active Control of Compressible Flows on a Curved Surface," Aerospace Technology Conference and Exposition. SAE Technical Paper 851856, Society of Automotive Engineers, Warrendale, PA, October 1985.
9. Maestrello, Lucio. "Active Transition Fixing and Control of the Boundary Layer in Air," AIAA Shear Flow Control Conference. Paper No. 85-0564, American Institute of Aeronautics and Astronautics, New York, March 1985.

10. Maestrello, Lucio and Lu Ting. "Analysis of Active Control by Surface Heating," AIAA 22nd Aerospace Sciences Meeting. Paper No. 84-0173, American Institute of Aeronautics and Astronautics, New York, January 1984.
11. Thomas, Andrew S. W. "The Control of Boundary-Layer Transition Using a Wave Superposition Principle," Journal of Fluid Mechanics, 137: 233-250 (1983)
12. Schlichting, Hermann W. Boundary Layer Theory. (Fourth Edition). New York: McGraw-Hill Book Co., 1960.
13. Shubauer, G. B. and H. K. Skramstad. "Laminar Boundary-Layer Oscillations and Stability of Laminar Flow," Journal of the Aeronautical Sciences, 14: 69-78 (February 1947).

Vita

Captain Lawrence Kudelka was born on 8 September 1956 in Trenton, New Jersey. He graduated from Steinert High School in 1974 and attended the United States Air Force Academy from which he received the degree of Bachelor of Science in Aeronautical Engineering in May 1978. Upon graduation, he received a commission in the USAF. He completed pilot training at Reese AFB, Texas and received his wings in November 1979. He then served as a C-141 pilot, instructor, and flight examiner in the 53rd Military Airlift Squadron, Norton AFB, California, until entering the School of Engineering, Air Force Institute of Technology, in June 1985.

Permanent address: 129 Grayson Avenue
Trenton, New Jersey 08619

UNCLASSIFIED

SECURITY CLASSIFICATION OF THIS PAGE

Handwritten notes or markings at the top right of the page.

REPORT DOCUMENTATION PAGE

1a. REPORT SECURITY CLASSIFICATION UNCLASSIFIED		1b. RESTRICTIVE MARKINGS None	
2a. SECURITY CLASSIFICATION AUTHORITY		3. DISTRIBUTION/AVAILABILITY OF REPORT Approved for public release; distribution unlimited.	
2b. DECLASSIFICATION/DOWNGRADING SCHEDULE			
4. PERFORMING ORGANIZATION REPORT NUMBER(S) AFIT/GAE/AA/86D-7		5. MONITORING ORGANIZATION REPORT NUMBER(S)	
6a. NAME OF PERFORMING ORGANIZATION School of Engineering	6b. OFFICE SYMBOL (If applicable) AFIT/ENY	7a. NAME OF MONITORING ORGANIZATION	
6c. ADDRESS (City, State and ZIP Code) Air Force Institute of Technology Wright-Patterson AFB, OH 45433-6583		7b. ADDRESS (City, State and ZIP Code)	
8a. NAME OF FUNDING/SPONSORING ORGANIZATION Structural Vibration Br. Flight Dynamics Lab.	8b. OFFICE SYMBOL (If applicable) AFWAL/FIBG	9. PROCUREMENT INSTRUMENT IDENTIFICATION NUMBER	
8c. ADDRESS (City, State and ZIP Code) AFWAL/FIBG Wright-Patterson AFB, OH 45433		10. SOURCE OF FUNDING NOS.	
11. TITLE (Include Security Classification) See box 19		PROGRAM ELEMENT NO.	PROJECT NO.
		TASK NO.	WORK UNIT NO.
12. PERSONAL AUTHOR(S) Lawrence Kudelka, B.S., Capt, USAF			
13a. TYPE OF REPORT MS Thesis	13b. TIME COVERED FROM _____ TO _____	14. DATE OF REPORT (Yr., Mo., Day) 1986 December	15. PAGE COUNT 72
16. SUPPLEMENTARY NOTATION			
17. COSATI CODES		18. SUBJECT TERMS (Continue on reverse if necessary and identify by block number)	
FIELD	GROUP	SUB. GR.	
01	03	Boundary Layer Transition	
20	04	Laminar Boundary Layer	
19. ABSTRACT (Continue on reverse if necessary and identify by block number)			
Title: BOUNDARY LAYER DISTURBANCES CAUSED BY PERIODIC HEATING OF A THIN RIBBON			
Thesis Advisor: Milton E. Franke, PhD Professor of Mechanical Engineering			
20. DISTRIBUTION/AVAILABILITY OF ABSTRACT UNCLASSIFIED/UNLIMITED <input checked="" type="checkbox"/> SAME AS RPT <input type="checkbox"/> DTIC USERS <input type="checkbox"/>		21. ABSTRACT SECURITY CLASSIFICATION UNCLASSIFIED	
22a. NAME OF RESPONSIBLE INDIVIDUAL Milton E. Franke, Professor		22b. TELEPHONE NUMBER (Include Area Code) 513-255-2362	22c. OFFICE SYMBOL AFIT/ENY

Approved for public release: LAW AFR 190-4
13 MAR 87
 Wright-Patterson AFB, OH 45433-6583
 Air Force Institute of Technology
 Department of Mechanical Engineering

Abstract

Wind tunnel experiments were conducted to generate velocity perturbations in a laminar boundary layer using periodic heating of a flush-mounted ribbon. A thin strip of Nichrome ribbon, flush-mounted on a flat plate, was heated by pulsed voltage of various frequencies with spring tension used to take up the slack caused by thermal expansion. Vibration of the ribbon was excited by the periodic thermal expansion and contraction due to the pulsed voltage. Sinusoidal velocity fluctuations were detected by a hot wire anemometer when the ribbon was allowed to vibrate during pulsed heating.

No effect on the amplitude of the flow disturbances was detected with the spring tension removed and segments of the ribbon firmly fixed to the surface such that no vibration of the ribbon occurred during periodic heating. Pulsed heating of a thin ribbon caused detectable flow disturbances only when the ribbon was allowed to vibrate.

The AFIT 9-in wind tunnel had sufficiently low turbulence to detect fluctuations when pulsed voltage was applied to the ribbon. Experiments conducted in the AFIT's 14-in wind tunnel were not able to show effects of heating because of the large amount of free-stream turbulence.

END

5-87

DTIC